Acta Biomaterialia 189 (2024) 192–207

Contents lists available at ScienceDirect

Acta Biomaterialia

journal homepage: www.elsevier.com/locate/actbio

Full length article

Type V collagen exhibits distinct regulatory activities in TMJ articular disc versus condylar cartilage during postnatal growth and remodeling

Prashant Chandrasekaran[a], Abdulaziz Alanazi[a], Bryan Kwok[a], Qing Li[a], Girish Viraraghavan[a], Sriram Balasubramanian[a], David B. Frank[b,c,d], X. Lucas Lu[e], David E. Birk[f], Robert L. Mauck[g,h], Nathaniel A. Dyment[g], Eiki Koyama[i], Lin Han[a,*]

[a] School of Biomedical Engineering, Science and Health Systems, Drexel University, Philadelphia, PA 19104, United States
[b] Penn-CHOP Lung Biology Institute, Perelman School of Medicine, University of Pennsylvania, Philadelphia, PA 19104, United States
[c] Penn Cardiovascular Institute, Perelman School of Medicine, University of Pennsylvania, Philadelphia, PA 19104, United States
[d] Division of Pediatric Cardiology, Department of Pediatrics, The Children's Hospital of Philadelphia, Philadelphia, PA 19104, United States
[e] Department of Mechanical Engineering, University of Delaware, Newark, DE 19716, United States
[f] Department of Molecular Pharmacology and Physiology, Morsani School of Medicine, University of South Florida, Tampa, FL 33612, United States
[g] McKay Orthopaedic Research Laboratory, Department of Orthopaedic Surgery, Perelman School of Medicine, University of Pennsylvania, Philadelphia, PA 19104, United States
[h] Translational Musculoskeletal Research Center, Corporal Michael J. Crescenz Veterans Administration Medical Center, Philadelphia, PA 19104, United States
[i] Department of Surgery, The Children's Hospital of Philadelphia, Philadelphia, PA 19104, United States

ARTICLE INFO

Article history:
Received 12 February 2024
Revised 2 September 2024
Accepted 26 September 2024
Available online 1 October 2024

Keywords:
Type V collagen
Temporomandibular joint
Fibrocartilage
Extracellular matrix
Mechanobiology

ABSTRACT

Understanding matrix molecular activities that regulate the postnatal growth and remodeling of the temporomandibular joint (TMJ) articular disc and condylar cartilage will enable the development of effective regenerative strategies targeting TMJ disorders. This study elucidated the distinct roles of type V collagen (collagen V) in regulating these two units. Studying the TMJ of young adult *Col5a1*$^{+/-}$ mice, we found that loss of collagen V resulted in substantial changes in the proliferation, clustering and density of progenitors in condylar cartilage, but did not have a major impact on disc cells that are more fibroblast-like. Although loss of collagen V led to thickened collagen fibrils with increased heterogeneity in the disc, there were no significant changes in local micromodulus, except for a reduction at the posterior end of the inferior side. Following the induction of aberrant occlusal loading by the unilateral anterior crossbite (UAC) procedure, both wild-type (WT) and *Col5a1*$^{+/-}$ condylar cartilage exhibited salient remodeling, and *Col5a1*$^{+/-}$ condyle developed more pronounced degeneration and tissue hypertrophy at the posterior end than the WT. In contrast, neither UAC nor collagen V deficiency induced marked changes in the morphology or biomechanical properties of the disc. Together, our findings highlight the distinct roles of collagen V in regulating these two units during postnatal growth and remodeling, emphasizing its more crucial role in condylar cartilage due to its impact on the highly mechanosensitive progenitors. These results provide the foundation for using collagen V to improve the regeneration of TMJ and the care of patients with TMJ disorders.

Statement of significance

Successful regeneration of the temporomandibular joint (TMJ) articular disc and condylar cartilage remains a significant challenge due to the limited understanding of matrix molecular activities that regulate the formation and remodeling of these tissues. This study demonstrates that collagen V plays distinct and critical roles in these processes. In condylar cartilage, collagen V is essential for regulating progenitor cell fate and maintaining matrix integrity. In the disc, collagen V also regulates fibril structure and local

* Corresponding author.
E-mail address: lh535@drexel.edu (L. Han).

https://doi.org/10.1016/j.actbio.2024.09.046

micromechanics, but has a limited impact on cell phenotype or its remodeling response. Our findings establish collagen V as a key component in maintaining the integrity of these two units, with a more crucial role in condylar cartilage due to its impact on progenitor cell activities.

1. Introduction

Temporomandibular joint (TMJ) is a diarthrodial joint responsible for everyday mandibular activities such as chewing and speaking [1]. Proper functioning of TMJ is endowed by the synergy of two loading counterparts, the articular disc and condylar cartilage [2]. TMJ disorders, a group of conditions that cause TMJ pain and dysfunction in jaw joint movement, afflicts 5-12% of the US population [3]. TMJ osteoarthritis (OA), a common subtype of TMD, is marked by progressive degeneration of cartilage tissues, subchondral bone remodeling and chronic inflammation in the joint, contributing to dysfunction of this loading pivot, reduced jaw motion and chronic pain [4]. Successful regenerative approaches could reestablish viable disc and condylar cartilage tissues that recapitulate their native extracellular matrix (ECM) structure and mechanical properties. This holds the potential for restoring TMJ function without inducing adverse complications including limited longevity, bone resorption and revision surgery, which are often caused by standard treatments such as prosthetics, autografts and viscosupplement administration [5,6]. One major roadblock, however, is the paucity of knowledge on the molecular activities that regulate the formation and degradation of the native ECM in these two tissues [7]. Articular disc contains a fibrous ECM dominated by type I collagen fibers with minute amount of proteoglycans [8]. This fibrous ECM has demonstrated a high degree of structural anisotropy and heterogeneity, with marked differences in fibril architecture and biomechanics across anterior, posterior, medial, lateral and central regions, and on superior versus inferior surfaces [9,10]. Condylar cartilage, on the other hand, consists of a hybrid ECM with a collagen I-dominated fibrocartilage layer covering a secondary collagen II-rich hyaline layer [11]. The matrix composition, structure and loading conditions of these two units are distinct from their two analog tissues in knee joint, the hyaline articular cartilage [12] and the fibrocartilaginous meniscus [13]. In contrast to the extensive studies on knee cartilage and meniscus, the structure-function relationships of the ECMs in the two TMJ tissues, along with their roles in joint function and disease are still poorly understood [14,15].

One key molecule that regulates the assembly of collagen I-based tissues is type V collagen (collagen V), a quantitatively minor fibril-forming collagen [16]. During embryonic and neonatal development, collagen V serves as the nucleation template to initiate collagen I fibrillogenesis [17] and limits aberrant fibril lateral growth via its partially processed N-propeptide [18]. The importance of collagen V in tissue health and function has been underscored by abnormal collagen fibril thickening, reduction of fibril numbers and impaired biomechanical properties in various collagen I-rich tissues such as skin [17], cornea [19], tendons and ligaments [20,21], which occur secondary to collagen V deficiency. In addition, deficiency of collagen V leads to reduced contraction and increased scar formation during wound healing in dermal [22,23] and cardiovascular [24] tissues. Classic Ehlers-Danlos Syndrome (cEDS) is a human genetic disorder (prevalence of ~ 1:20,000) due to the mutation or haploinsufficiency of *COL5A1* or *COL5A2* gene [25]. These cEDS patients show higher propensity toward TMD [26], indicating the importance of collagen V in human TMJ health. Indeed, our recent study found that in murine models of collagen V deficiency, the condylar cartilage developed thickened collagen fibrils, reduced modulus, decreased cell density and aberrant cell clustering in both the fibrous and hyaline layers [27]. Meanwhile, despite its well-recognized structural role [17,18], even in collagen I-dominated tissues, the presence and activities of collagen V vary substantially with tissue type, location and age [28]. Although the disc shares the dominance of collagen I fibrils as the condylar cartilage fibrous layer [8], it is unclear whether collagen V is also a crucial matrix constituent therein, or how its activities may vary with the pronounced spatial heterogeneity within the disc. Furthermore, since the growth, maintenance and pathology of TMJ is highly sensitive to occlusal loading [29-32], it is also important to elucidate how collagen V impacts the response of these two tissues under non-physiologic loading-induced remodeling. Such knowledge could provide novel insights into the pathology and mechanobiology of human TMJ OA, while also improving the understanding and care for cEDS patients.

The objective of this study was to delineate the contributions of collagen V to the structure and function of articular disc versus condylar cartilage, and separate its roles in regulating normal postnatal growth and aberrant loading-induced remodeling *in vivo*. To query the impact of collagen V deficiency on the postnatal growth of articular disc, we assessed its morphology, cellularity, collagen fibril nanostructure and biomechanical properties in the cEDS murine model ($Col5a1^{+/-}$ [17]) at 3 months of age. To determine the age-dependent impact of collagen V loss on the disc postnatal growth, we tested the inducible collagen V knockout mice ($Col5a1^{iKO}$ [19]). In these mice, we maintained the normal level of collagen V in embryonic and neonatal development, induced the knockout of *Col5a1* gene expression at 1 week (pre-weaning) and 1 month (post-weaning) of ages, and analyzed the resulting disc phenotype at 1 and 2 months, respectively. The structural and biomechanical phenotype of disc was interpreted within the context of collagen V distribution, matrix structure and cell phenotype, and was compared to the phenotype of condylar cartilage [27] to differentiate the activities of collagen V in these two units. Next, given the high mechanosensitivity of TMJ [29-32], we applied the unilateral anterior crossbite (UAC) prosthesis model to induce aberrant occlusal loading *in vivo* [33,34]. Analyzing structural and mechanical changes of both tissues in $Col5a1^{+/-}$ and wild-type (WT) mice, we examined whether the two units have different remodeling responses to altered loading, and whether collagen V has differential impacts to each tissue in this process. Our findings highlight that collagen V plays distinct roles in regulating the integrity of TMJ condylar cartilage and articular disc, both during postnatal growth and under UAC-induced remodeling. Meanwhile, results underscore specific characteristics in the matrix organization and cell fate of these two distinct fibrocartilaginous tissue units.

2. Methods

2.1. Animal model

Collagen V deficient murine models, including $Col5a1^{+/-}$ and $Col5a1^{iKO}$ ($Col5a1^{flox/flox}/Rosa26Cre^{ER}$) mice in the C57BL/6 strain, were generated as previously described [17,19] and housed in

the Calhoun animal facility at Drexel University. Age-matched, 3-month-old *Col5a1*$^{+/-}$ and WT littermates were sacrificed for histological, nanostructural and biomechanical analyses. To induce postnatal ablation of *Col5a1* gene in the *Col5a1*^{iKO} model, tamoxifen (T5648, Sigma) was intraperitoneally (i.p.) injected to mice at 4.5 mg per 40 g of body weight per day for 3 consecutive days in the form of 20 mg/mL suspension in sesame oil (S3547, Sigma) with 1% benzyl alcohol (305197, Sigma). By day 5, the excision of *Col5a1* expression in the TMJ was confirmed by qPCR (forward primer: 5'-AAGCGTGGGAAACTGCTCTCCTAT-3', reverse primer: 5'-AGCAGTTGTAGGTGACGTTCTGGT-3'). The knockout was induced at 1 week and 1 month of age, and mice were sacrificed at 1 and 2 months of age, respectively. Two control groups were used, including *Col5a1*$^{flox/flox}$/*Rosa26Cre*^{ER} mice injected with vehicle (the same amount of sesame oil and benzyl alcohol but without tamoxifen) and WT mice injected with tamoxifen at the same dosage and frequency. Based on histological and biomechanical analyses, we found no significant differences between these two groups. We found no significant differences between male and female mice, and thus, both sexes were included here. Also, for both *Col5a1*$^{+/-}$ and *Col5a1*^{iKO} mice used here, we did not notice appreciable changes in body weight, size, increased incidents of bone fracture or other whole-body abnormalities. For all the experiments, except for the UAC procedure, approximately equal numbers of animals from each sex were used ($n = 2$ or 3 from each sex to yield $n = 5$ to 6 for each genotype/group).

To induce aberrant occlusal loading, the UAC prosthesis was applied to female *Col5a1*$^{+/-}$ and WT mice at 3 months of age, following the established procedure [34]. In brief, metal tubes (1 mm inner diameter, 0.2 mm thickness, Shinva Ande, Shandong, China) were bonded to the left maxillary and mandibular incisors using dental Zinc cement to create a unilateral crossbite relationship. The mandibular tubes for the top left incisors were 1.5 mm long, while tubes for the bottom incisors were curved to form 135° labially inclined occlusal plate. These prostheses were attached to the left incisors of each mouse under anesthesia induced by i.p. injections of a mixture of ketamine (Vedco, 85 mg/kg body weight) and xylazine (Akorn Animal Health, 15 mg/kg body weight). For the Sham group, similar prostheses were attached to the top and bottom incisors, but without the dental cement. With minimal postoperative care, the mice were fed with the standard pellet diet (12.5 mm in diameter and 15-20 mm in length, PicoLab 5053, Animal Specialties and Provision) for three weeks. At the end of week three, mice were euthanized and TMJs were harvested for subsequent histological, nanostructural and biomechanical analyses. To ensure consistency, all the analyses were performed on the left TMJ, following the established procedure [34]. All animal work was approved by the Institutional Animal Care and Use Committee (IACUC) at Drexel University.

2.2. Histology and immunofluorescence imaging

Murine TMJs were fixed in 4% paraformaldehyde in PBS (Santa Cruz Biotech) for 24 hrs, and decalcified in 10% ethylenediaminetetraacetic acid (EDTA, pH ≈ 7.4, E9884, Sigma) over 21 days. Six µm-thick serial sagittal sections were obtained and every fifth section was stained with Hematoxylin & Eosin (H&E) or Safranin-O/Fast Green to assess tissue morphology, cellularity, cell morphology and gross-level sGAG staining of the TMJ ($n \geq 5$ animals for each staining). For TMJs of 3-month-old WT and *Col5a1*$^{+/-}$ mice, the cell density and cell nuclear aspect ratio (NAR) were quantified for each tissue using H&E images. Also, for TMJs of WT and *Col5a1*$^{+/-}$ mice subjected to UAC and Sham procedures, the cell density of each tissue and the thickness of each condylar cartilage layer were quantified. For each image, a region of interest (ROI, 200 × 100 µm^2) was identified to define the anterior, central, and posterior regions of TMJ, and to separate articular disc, condylar fibrous and hyaline layers. In each ROI, the cell density and NAR were measured using ImageJ (FIJI). To assess the impact of aberrant occlusal loading on TMJ remodeling, morphological and biochemical changes in the condyle of UAC and Sham groups were scored based on the modified Mankin Scoring system for TMJ condylar cartilage by two blinded observers (BK and GV), including the metrics of pericellular Safranin-O staining (0-2), background Safranin-O staining (0-3), chondrocyte arrangement (0-2) and cartilage structural integrity (0-3) [35].

For immunofluorescence (IF) imaging of collagen V, additional sections were incubated with Bloxall (SP-6000, Vector Laboratories) to quench endogenous peroxidases and phosphatases activities, and stained with anti-collagen V antibody (AB7046, Abcam, 1:100 dilution) overnight at 4°C, and then, incubated with AlexaFlour 488 nm goat anti-rabbit secondary antibody (A-11037, Invitrogen, 1:250). For Ki-67, the cell proliferation biomarker [36], and β-catenin, sections from 1-month-old *Col5a1*^{iKO} (following the induced ablation of *Col5a1* gene at 1 week of age) and control mice were first incubated with primary antibody (Ki-67, 550609, BD Pharmigen, 1:50 dilution; β-catenin: 610153, BD Pharmigen, 1:50) overnight, followed by HRP horse anti-mouse IgG (MP-7402, Vector Labs) for 1 hr, and then, stained with TSA fluorescein reagent (SAT701001EA, Akoya Biosciences) for 8 min. We focused our Ki-67 and β-catenin analysis on 1-month-old *Col5a1*^{iKO} and control TMJs given that collagen V was known to have a more profound impact on matrix assembly and cell activities during early development and growth [17,27]. IF images were taken with a Leica DM6000B Live Imaging Microscope or Leica DMi8 Confocal Microscope (Leica Microsystems, $n \geq 5$ for each staining). For all images, sections incubated without the primary antibody but with the secondary antibody were included as internal negative controls to confirm specificity. The percentage of Ki-67(+) cells were quantified by the "spots" function in IMARIS (Bitplane, Oxford Instruments, Version 9.7.2), which rendered spherical spots to every cell and allowed us to identify the number of Ki-67(+) versus total cells via DAPI. The relative intensity of β-catenin staining was estimated using the "surface" function in IMARIS for area reconstruction of β-catenin positive cells, which was then normalized to the total tissue area acquired based on DAPI channel using the "area statistics" function.

2.3. Collagen nanostructural analysis

Scanning electron microscopy (SEM) was applied to visualize and quantify the collagen fibril structure on the surfaces of condylar cartilage, disc superior and inferior sides, following the established procedure [10]. In brief, immediately after AFM-nanoindentation, TMJ condyles and discs were processed for proteoglycan removal, fixed and dehydrated, air dried overnight, coated with ≈ 6 nm thick platinum-palladium mixture, and then, imaged using a Supra 50 VP SEM (Carl Zeiss). We then quantified collagen diameters using ImageJ (FIJI, 350 fibrils, $n = 3$ animals for each group).

2.4. AFM-based nanoindentation

AFM-nanoindentation was performed on the surfaces of freshly dissected TMJ discs using custom-made microspherical colloidal tips ($R \approx 5$ µm, nominal $k \approx 2$ N/m, NSC36-B, NanoAndMore) and a Dimension Icon AFM (Bruker Nano) at ≈ 10 µm/s rate in 1× PBS with protease inhibitors (Pierce 88266, ThermoFisher), following our established procedure [10,37] ($n \geq 5$). In addition, for TMJs subjected to UAC and Sham procedures, AFM-nanoindentation was performed on both the disc and central region of condylar cartilage ($n = 5$). For each side of the disc, nanoindentation was performed on the anterior, central and posterior regions to assess regional

heterogeneity. For each sample and each region, at least 10-15 locations were tested to account for local spatial heterogeneity. The indentation modulus, E_{ind}, was calculated by fitting the entire loading portion of the *F-D* curve with finite thickness-corrected Hertz model [38], assuming Poisson's ratio $\nu \approx 0$ for both the disc [39] and condylar cartilage [40].

2.5. Statistical analysis

The linear mixed model was applied to analyze cell density, NAR, thickness of each condylar cartilage layer, d_{col}, E_{ind}, percentage of Ki-67+ cells as well as relative intensity of β-catenin staining using the R package lme4 (version1.1-35) [41]. In these tests, genotype (WT versus *Col5a1*$^{+/-}$, or control versus *Col5a1*^{iKO}), procedure (UAC versus Sham), tissue sides (superior versus inferior), regions (anterior, central and posterior) and layers (articular disc, condylar fibrous and hyaline layers) were treated as fixed effect factors when appropriate, and individual animal was treated as a random effect factor when applicable, with interaction terms between the fixed effects. Likelihood ratio test was applied to determine the choice of two covariance structures, unstructured versus compound symmetry. To account for family-wise type I errors, Tukey-Kramer post-hoc multiple comparison was applied to calculate adjusted *p*-values for comparisons amongst different tissue layers or regions, and Holm-Bonferroni multiple contrast correction [42] was applied to calculate the adjusted *p*-values for comparisons between genotypes, procedures and articular disc tissue sides. For the semi-quantitative modified Mankin scores, non-parametric Mann-Whitney U test was applied, followed by Holm-Bonferroni multiple contrast correction for comparisons between genotypes and procedures. For the variance of d_{col}, unpaired two-sample *F*-test was applied, followed by Holm-Bonferroni multiple contrast correction for comparisons between genotypes, procedures, regions and disc sides. In all the tests, the significance level was set at $\alpha = 0.05$. A complete list of all quantitative and statistical outcomes were summarized in Tables S1–S10.

3. Results

3.1. Impact of collagen V reduction on the cell density and nucleus morphology of articular disc versus condylar cartilage

In the articular disc of 3-month-old WT mice, collagen V was found to be mainly present in the pericellular domain, with a concentration lower than that in the condylar fibrous layer (Fig. 1a). In *Col5a1*$^{+/-}$ mice, as expected, staining of collagen V was reduced in both the disc and condylar cartilage, validating decreased collagen V content in this heterozygous model. Given its lower presence in the disc, the extent of collagen V reduction was also less pronounced compared to that in condylar fibrous layer (Fig. 1a).

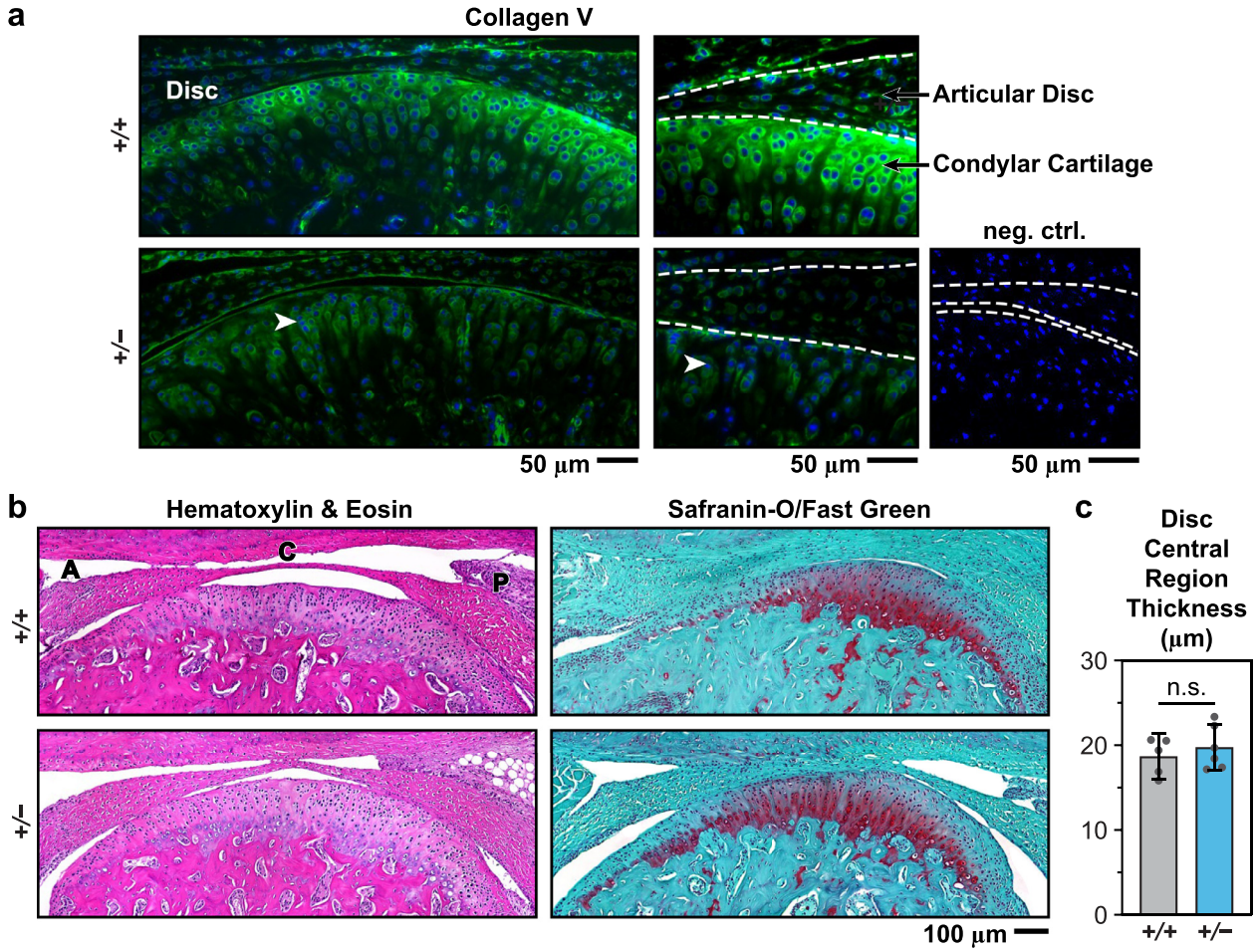

Fig. 1. a) Immunofluorescence (IF) images of collagen V show the distribution of collagen V in the TMJ articular disc and condylar cartilage of 3-month-old wild-type (+/+) and *Col5a1*$^{+/-}$ (+/–) mice. b) Hematolyxin & Eosin (H&E) and Safranin-O/Fast Green (Saf-O) histology images show the overall morphology and sulfated glycosaminoglycan (sGAG) distribution (A: anterior, C: central, P: posterior). c) Comparison of articular disc thickness in the central region between +/+ and +/– TMJs (mean ± 95% CI, $n = 5$, n.s.: not significant). Each data point represents the average value measured from one animal.

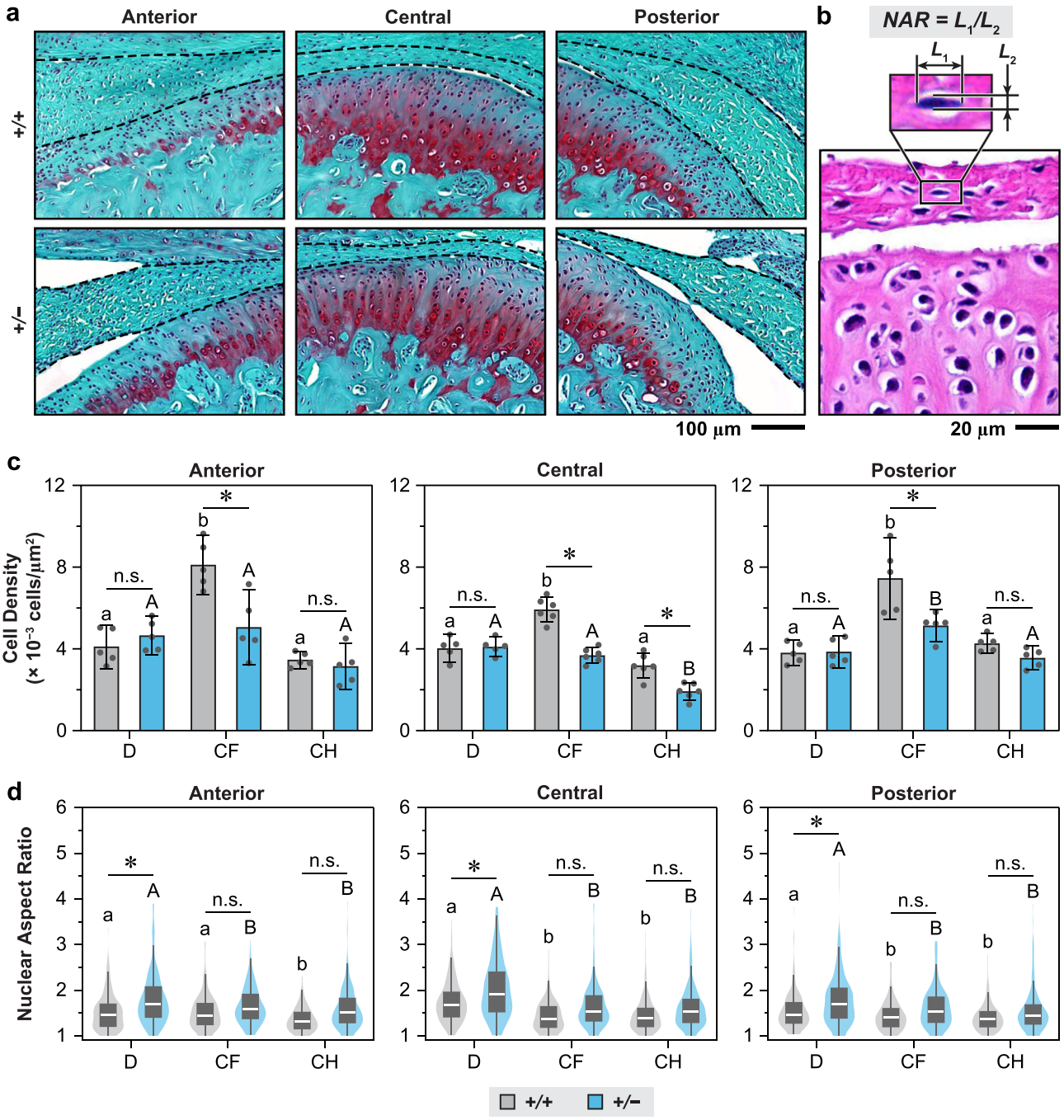

Fig. 2. Impact of collagen V reduction on the cell density and nuclear aspect ratio (NAR) of TMJ articular disc and condylar cartilage. a) Safranin-O/Fast Green histology images of 3-month-old wild-type (+/+) and *Col5a1*$^{+/-}$ (+/−) TMJs show no appreciable differences in joint morphology or sGAG staining across the anterior, central and posterior regions. Dashed lines denote the boundary of articular disc. b) Zoom-in H&E histology image of *Col5a1*$^{+/-}$ TMJ illustrates the definition of NAR. c) Cell density (mean ± 95% CI) and d) violin plots of cell NAR for the disc (D), condylar cartilage fibrous (CF) and hyaline (CH) layers across the anterior, central and posterior regions (*: $p < 0.05$, n.s.: not significant, different letters indicate significant differences between different layers within each region for each genotype). A complete list of statistical analysis outcomes for cell density and NAR is summarized in Tables S1 and S2, respectively.

At the histological level, reduction of collagen V did not lead to appreciable changes in the overall TMJ morphology (Fig. 1b). For instance, the central region of the disc had similar thickness between WT (19 ± 3 μm, mean ± 95% CI, $n \geq 5$) and *Col5a1*$^{+/-}$ TMJs (20 ± 3 μm, $p = 0.485$ via unpaired two-sample student's *t*-test, Fig. 1c). For condylar cartilage, following our previous study reporting no significant differences in the thickness of each tissue layer and sGAG staining in the central region [27], here we further showed that there were also no salient changes at the anterior and posterior ends (Figs. 1b and 2a), suggesting that the overall condylar morphology was not impacted by the haploinsufficiency of collagen V during postnatal growth.

We found the impact of collagen V reduction on cell density to be different for articular disc versus condylar cartilage (Fig. 2a-c). For the disc, we did not find significant differences in cell densities between WT and *Col5a1*$^{+/-}$ TMJs across the anterior, central and posterior regions (Fig. 2c). This was distinct from changes in condylar cartilage, in which, *Col5a1*$^{+/-}$ fibrous layer showed significantly lower cell densities throughout all three regions than the WT, and hyaline layer also had reduced density in the cen-

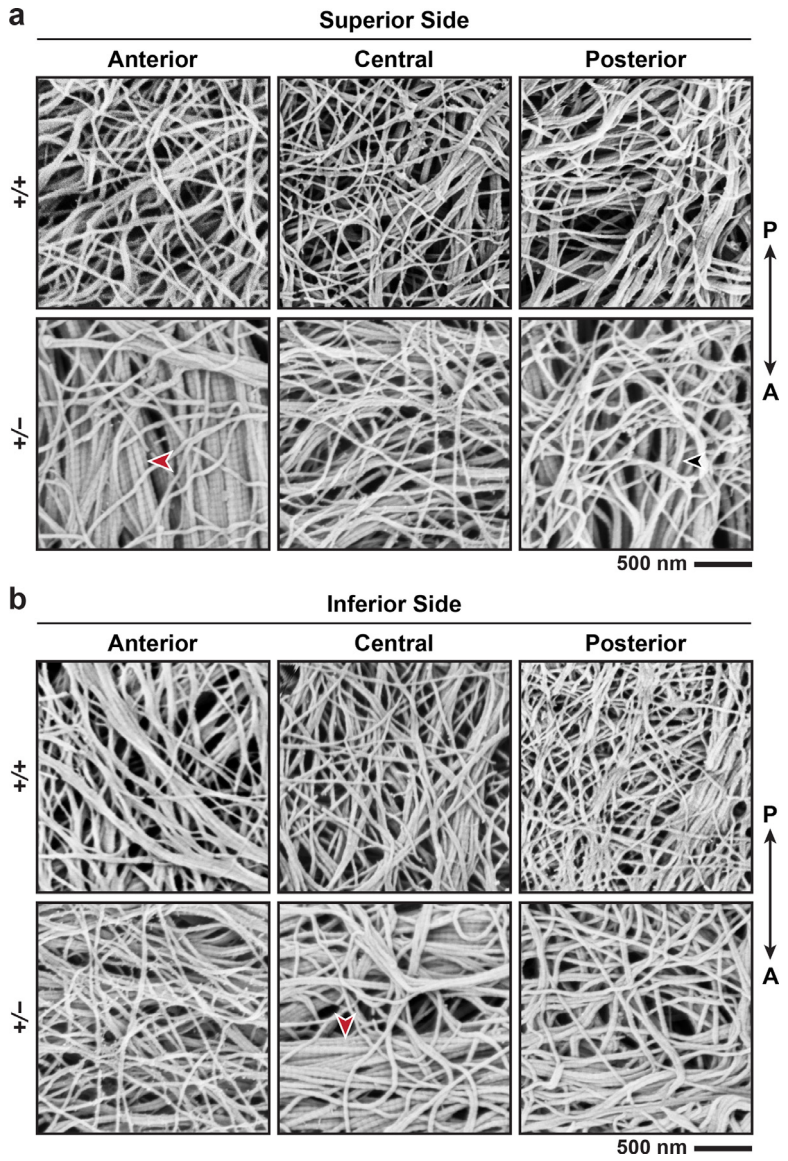

Fig. 3. Representative SEM images of the surfaces of TMJ articular disc from 3-month-old wild-type (+/+) and *Col5a1*$^{+/-}$ (+/–) mice, a) superior side, b) inferior side (A: anterior, P: posterior). Red arrowheads: D-band periodicity typically found in mature, thicker collagen fibrils.

tral region. Meanwhile, in WT TMJ, cell densities were significantly higher in the condylar fibrous layer than those in the hyaline layer or disc, with the latter two being similar throughout all three regions (Fig. 2c). In contrast, in *Col5a1*$^{+/-}$ TMJ, the condylar fibrous layer and disc had similar cell densities in anterior and central regions, while the fibrous layer showed higher cell densities than hyaline layer in central and posterior regions (Fig. 2c). In addition, cells in the disc adapted a more elongated nuclear morphology than those in condylar cartilage, as marked by significantly higher NARs (Fig. 2d). Such contrast was consistent across all three regions for both genotypes, except for the anterior region of WT TMJ, where the disc and condylar fibrous layer had similar NARs (Fig. 2d). Comparing the two genotypes, cells in *Col5a1*$^{+/-}$ disc showed significantly higher NARs in all tissue layers throughout all three regions, while there were no genotype-associated differences in condylar cartilage NARs (Fig. 2d). Performing Pearson's correlation analysis between cell density and the average NAR from each region and layer, we did not find significant correlation between these two parameters (r = -0.039 [-0.328 0.258], p = 0.802 for WT, and r = 0.065 [-0.233 0.352], p = 0.672 for *Col5a1*$^{+/-}$).

3.2. Impact of collagen V reduction on the fibril nanostructure and biomechanics of articular disc versus condylar cartilage

At the nanoscale, reduction of collagen V resulted in significant changes in the collagen fibril nanostructure of disc ECM. For both genotypes, on both the superior and inferior disc surfaces, we observed a mixture of individual, random fibrils entangled with aligned fibril bundles (Fig. 3). This was different from the condylar cartilage surface, which was dominated by random collagen fibril meshes [27], highlighting distinct structural traits of these two tissues. In comparison to the WT, *Col5a1*$^{+/-}$ disc exhibited a more salient presence of aligned fibril bundles, which also displayed the characteristic D-band periodicity [43] usually found in thicker fibrils (Fig. 3, red arrowheads). Indeed, *Col5a1*$^{+/-}$ disc had significantly larger fibril diameter, d_{col}, with a higher heterogeneity (variance of d_{col}) than the WT disc (Fig. 4a,b). This thickening effect was present throughout anterior, central and posterior regions, and on both superior and inferior surfaces. Meanwhile, the degree of increase in the average and heterogeneity of d_{col} was more pronounced on the superior surface of *Col5a1*$^{+/-}$ disc (Fig. 4a,b).

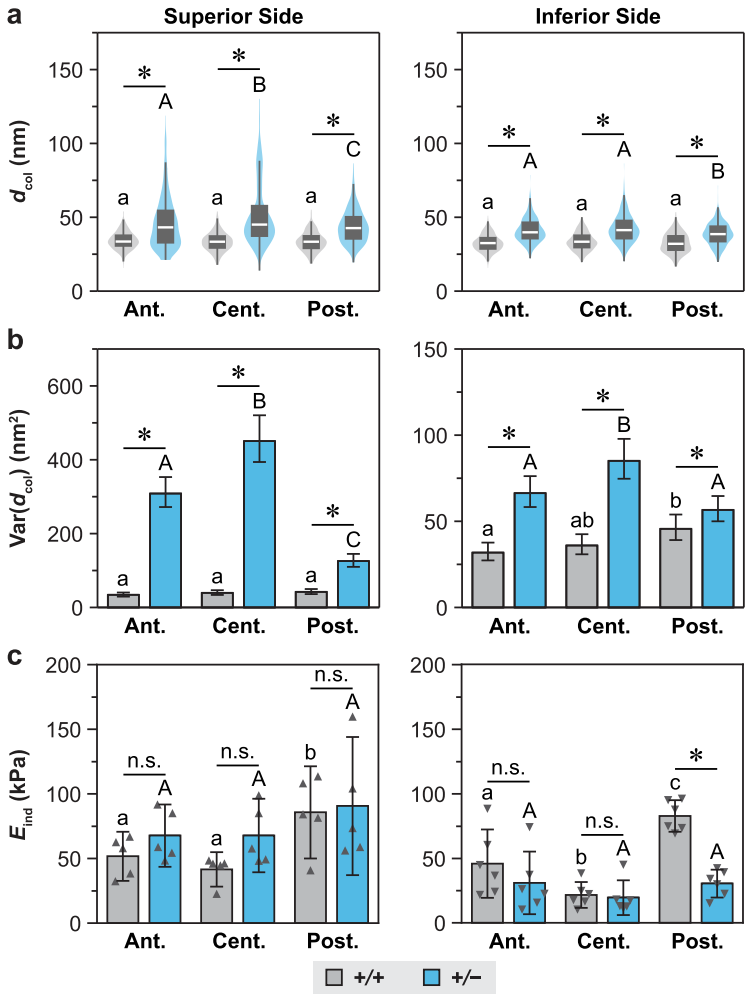

Fig. 4. Impact of collagen V reduction on the surface collagen fibril nanostructure and biomechanics of TMJ articular disc. a,b) Comparisons of a) collagen fibril diameter, d_{col}, distribution (violin plots) and b) heterogeneity (variance, mean ± 95% CI) between 3-month-old wild-type (+/+) and *Col5a1*$^{+/-}$ (+/–) discs (> 150 fibrils from $n = 3$ mice for each genotype, region and surface side). c) Comparison of indentation modulus, E_{ind} (kPa), between genotypes (mean ± 95% CI, $n = 5$, *: $p < 0.05$, n.s.: not significant, different letters indicate significant differences between different regions on each side of the disc for each genotype). Each data point represents the average value measured from one animal. A complete list of statistical analysis outcomes for d_{col} and E_{ind} is summarized in Tables S3 and S4, respectively.

As a result, in WT disc, fibrils on the superior and inferior sides have similar diameters, while in *Col5a1*$^{+/-}$ disc, fibrils on the superior side were significantly thicker than those on the inferior side (Fig. 4a,b and Table S3).

Applying AFM-based nanoindentation, we found that the impact of collagen V reduction on articular disc micromechanics varied markedly with tissue regions (Fig. 4c). On the inferior side, *Col5a1*$^{+/-}$ disc showed substantially lower modulus at the posterior end compared to the WT (31 ± 11 kPa versus 83 ± 12 kPa, $p < 0.001$, $n = 6$). However, we did not find significant genotype-associated differences in other regions or on the superior side. Meanwhile, these two genotypes showed different regional heterogeneity in E_{ind}. For WT disc, the posterior ends had higher modulus than the central and anterior regions on both superior and inferior sides, consistent with our previous study [10]. In contrast, for *Col5a1*$^{+/-}$ disc, we found no significant regional variations (Fig. 4c).

3.3. Impact of induced collagen V ablation on the postnatal growth of articular disc in *Col5a1*^{iKO} mice

In the *Col5a1*^{iKO} model, after the induced *Col5a1* ablation at 1 week and 1 month of age, we did not notice salient morphological changes of the disc at either 1 or 2 months, respectively (Fig. 5a), similar to the observation in 3-month-old *Col5a1*$^{+/-}$ mice (Figs. 1, 2a). For 1-month-old *Col5a1*^{iKO} disc, there was a significant reduction of E_{ind} at the posterior end on both sides. At 2 months of age, we noted marked reduction of E_{ind} at the posterior end on the superior side, but no changes on the inferior side (Fig. 5b). Overall, similar to that of *Col5a1*$^{+/-}$ disc (Fig. 4c), reduction of collagen V led to decreased local micromodulus of the disc, but the impact was heterogeneous across different regions and tissue sides. These phenotypic changes again illustrated more varied and moderate developmental defects in the disc comparing to condylar cartilage, in which, we found not only significant modulus reduction but also clear morphological changes, including a substantial thinning of the hyaline layer in 2-month-old *Col5a1*^{iKO} condylar cartilage (black arrowhead, Fig. 5a) [27].

In 1-month-old *Col5a1*^{iKO} mice, immunostaining for Ki-67 demonstrated that the disc and condylar cartilage cells exhibited distinct proliferation activities and responses to collagen V ablation (Fig. 6a). In condylar cartilage, the control mice showed appreciable nuclear staining of Ki-67 in the fibrous layer cells across anterior, central and posterior regions, and such staining was much reduced in all three regions of the *Col5a1*^{iKO} condyle (Fig. 6b). This suggested that cells in the fibrous layer undergo active proliferation at the postnatal age of 1 month, and that ablation of *Col5a1*

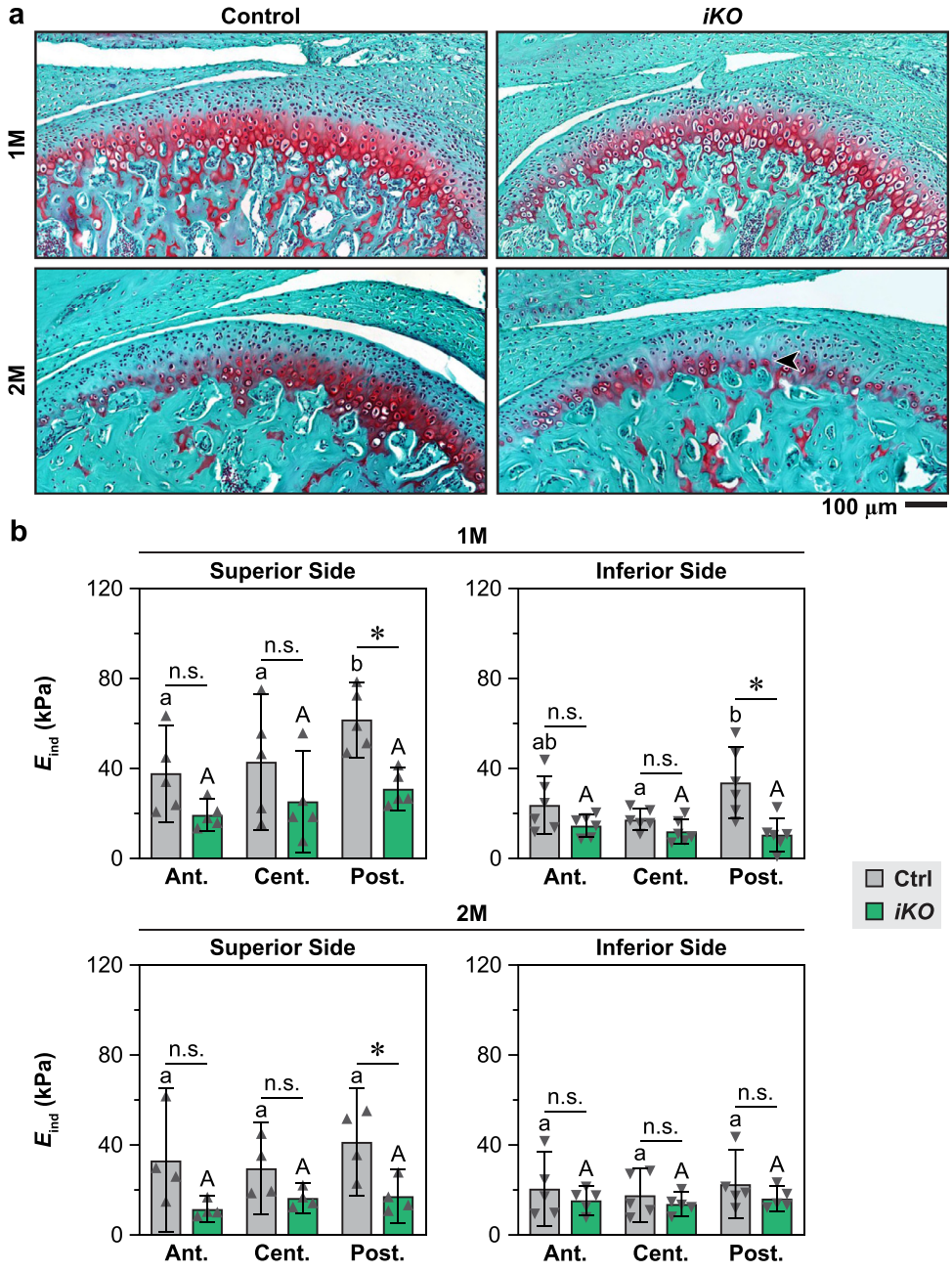

Fig. 5. Impact of induced collagen V ablation on the postnatal growth of TMJ articular disc. a) Safranin-O/Fast Green histology images show the morphology and sGAG staining of the control and *Col5a1*^{iKO} (*iKO*) TMJs at 1 month (ablation of *Col5a1* gene via TM injection at 1 week of age) and 2 months (ablation at 1 month) of age, respectively. b) Comparison of indentation modulus, E_{ind} (kPa), of articular disc between the control and *iKO* mice across anterior, central and posterior regions on both superior and inferior sides (mean ± 95% CI, $n = 5$, *: $p < 0.05$, n.s.: not significant, different letters indicate significant differences between different regions on each side of the disc for each genotype). Each data point represents the average value measured from one animal. A complete list of statistical analysis outcomes for E_{ind} is summarized in Tables S4.

in neonatal mice led to reduced cell proliferation at 1 month [27]. In contrast, in the disc, we did not detect appreciable signals of Ki-67 for either control or *Col5a1*^{iKO} mice (Fig. 6a), suggesting that, unlike condylar cartilage progenitors, disc cells have likely lost their proliferative capabilities by 1 month of age. In addition, we detected pronounced staining of β-catenin in the fibrous layer of condylar cartilage (Fig. 6c), consistent with our previous study showing active Wnt/β-catenin activities in these progenitors [27]. There was also a significant reduction in the β-catenin expression in *Col5a1*^{iKO} condyle throughout all three regions (Fig. 6d), corroborating the reduction of Ki-67 activities. Similarly, we noted very low expression of β-catenin in disc cells for both genotypes (Fig. 6c), further illustrating the distinct fate of disc cells compared to condylar progenitors.

3.4. Impact of collagen V reduction on condylar cartilage remodeling under aberrant occlusal loading

In response to the UAC-induced altered occlusal loading, condylar cartilage underwent salient remodeling and structural changes by 3 weeks. In WT condyle, UAC-operation resulted in reduced sGAG staining and hyaline layer thickness, as well as lower cell densities in both fibrous and hyaline layers in the central region (Fig. 7), consistent with the literature [34]. In *Col5a1*$^{+/-}$ condyle,

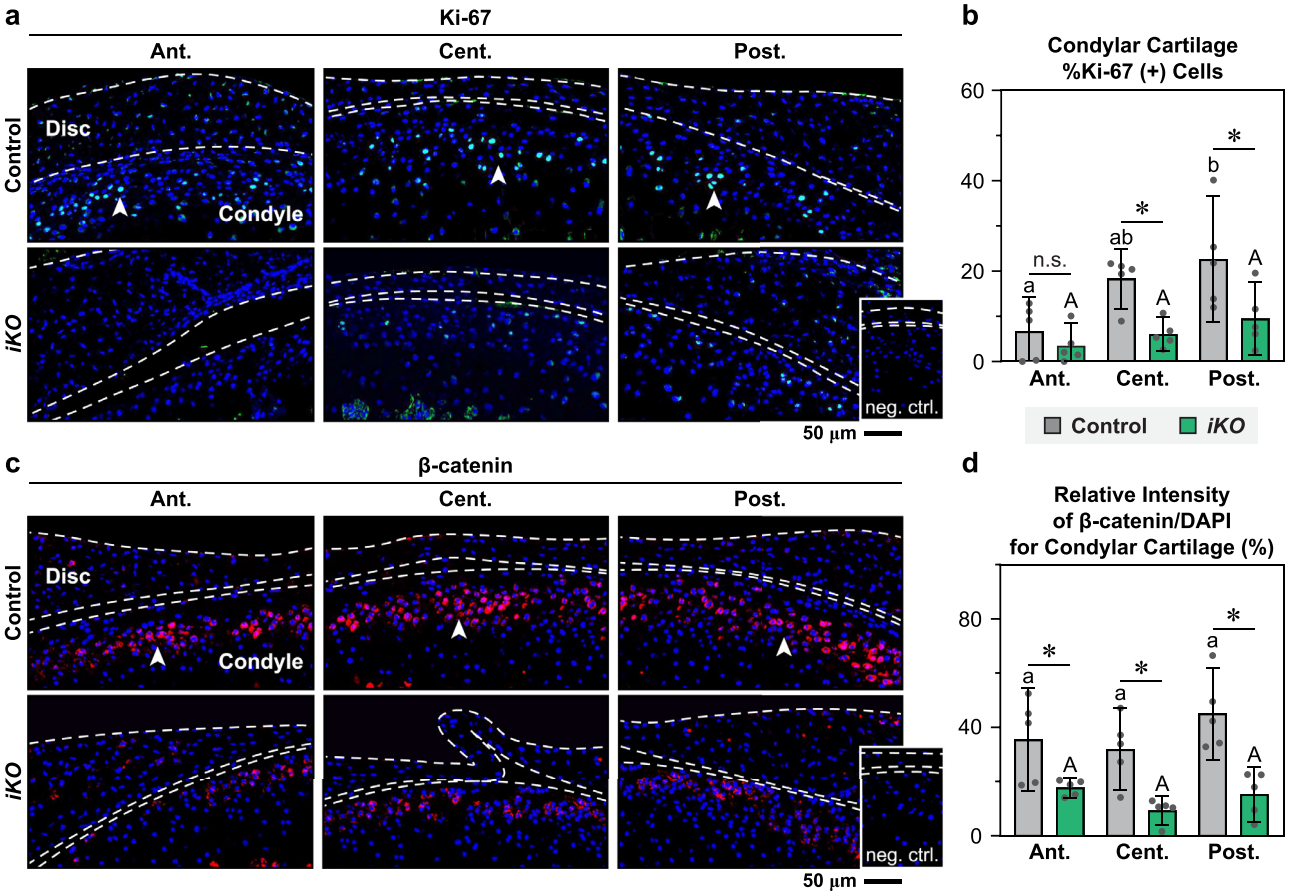

Fig. 6. Impact of induced collagen V ablation on the expression of Ki-67 and β-catenin in TMJ articular disc and condylar cartilage. a,c) Immunofluorescence (IF) images of the control and *Col5a1*^{iKO} (*iKO*) TMJs show appreciable staining of a) Ki-67 and c) β-catenin in the condylar cartilage fibrous layer across all three regions (white arrowheads), but not in the disc, as well as reduced staining in *iKO* condylar cartilage at 1 month of age (ablation of *Col5a1* gene via TM injection at 1 week of age). b,d) Comparisons of b) the percentage of Ki-67-positive cells, %Ki-67 (+), and d) relative intensity of β-catenin/DAPI staining in the condylar cartilage of 1-month-old control and *iKO* mice (mean ± 95% CI, $n = 5$, *: $p < 0.05$ between genotypes, n.s.: not significant, different letters indicate significant differences between different regions for each genotype). Each data point represents the average value measured from one animal. A complete list of statistical analysis outcomes for %Ki-67(+) cells and relative intensity of β-catenin is summarized in Table S5.

we found reduced thicknesses for both fibrous and hyaline layers, but no significant changes in cell densities. In addition, for both genotypes, the posterior end of condylar cartilage developed increased sGAG staining and thickening for both fibrous and hyaline layers (Figs. 7b, 8a). Comparing the two genotypes, the UAC procedure resulted in more pronounced thickening of hyaline layer at the posterior end for *Col5a1*$^{+/-}$ condyle, as marked by its significantly higher hyaline layer thickness than UAC-operated WT condyle (Figs. 7b, 8a). In addition, in the central region, the fibrous layer of *Col5a1*$^{+/-}$ condyle showed lower cell density than WT for the Sham group, but had similar cell densities for the UAC group. At the posterior end, however, *Col5a1*$^{+/-}$ condyle fibrous layer had lower cell densities than the WT for both Sham and UAC groups (Fig. 8b). We did not notice appreciable changes in condylar thickness or cell densities at the anterior end after UAC (Fig. 8). Evaluating changes in sGAG staining, chondrocyte arrangement and cartilage structure [35], we found significantly higher modified Mankin scores for UAC-operated condyles than the Sham control for both genotypes (Fig. 7c), illustrating salient remodeling and degeneration. Meanwhile, UAC-operated *Col5a1*$^{+/-}$ condyles had higher Mankin scores (4.6 ± 1.2, mean ± 95% CI, $n = 5$) than the WT (2.9 ± 0.5, $p = 0.009$), supporting that deficiency of collagen V increased the susceptibility of condylar cartilage to aberrant loading.

In addition to the histological phenotype, we also found marked changes in the surface collagen fibril nanostructure and mechanical properties of condylar cartilage following UAC. For both genotypes, condylar cartilage retained the transverse random fibril architecture (Fig. 9a), indicating that the UAC model induced minimal surface fibrillation by 3 weeks, which was marked by the formation of aligned collagen fibril bundles [44]. On the other hand, UAC resulted in significant increases in both the average (Fig. 9b) and heterogeneity (variance) (Fig. 9c) of d_{col} for WT cartilage surface, but only a trend of increase in the variance of d_{col} for *Col5a1*$^{+/-}$ cartilage ($p = 0.067$). On the mechanics front, UAC led to a significant modulus reduction for both WT ($p < 0.0001$) and *Col5a1*$^{+/-}$ condylar cartilage ($p = 0.023$, Fig. 9d). Comparing the two genotypes, *Col5a1*$^{+/-}$ condylar cartilage showed higher average and heterogeneity of d_{col} than the WT for the Sham group, but not the UAC group, and had a lesser degree of changes in the average and variance of d_{col} in response to UAC (Fig. 9b,c). Also, for the Sham group, the modulus of *Col5a1*$^{+/-}$ condylar cartilage was lower than that of WT ($p < 0.0001$), while for the UAC group, no genotype-associated differences were observed ($p = 0.494$, Fig. 9d).

3.5. Differential responses of articular disc to aberrant occlusal loading and collagen V reduction

In contrast to the pronounced remodeling of condylar cartilage, UAC did not result in salient changes in morphology, cell density or the presence of sGAGs in the articular disc of both genotypes

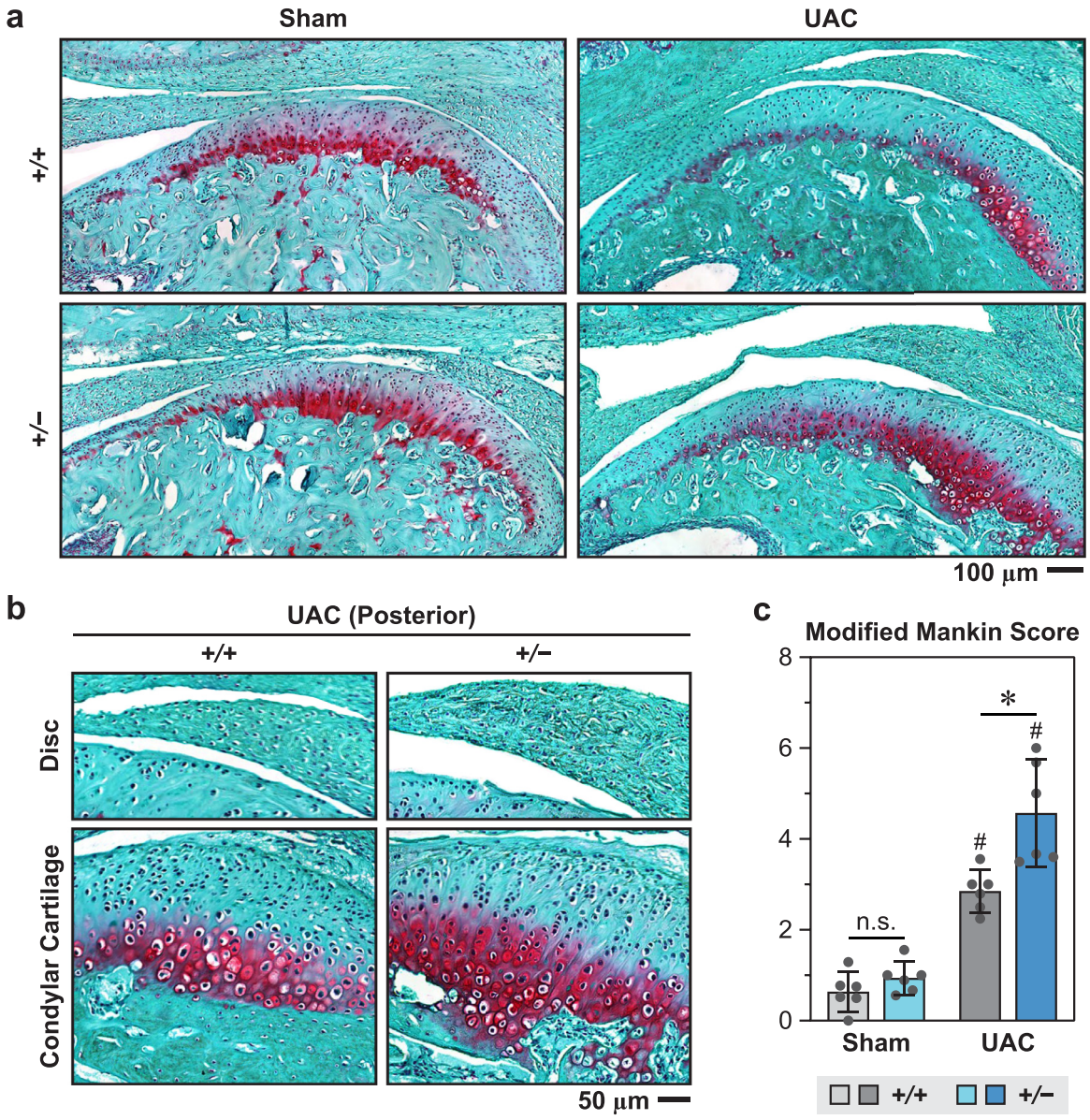

Fig. 7. Remodeling of TMJ condyle at 3 weeks after the unilateral anterior crossbite (UAC) prosthesis model. a) Representative Safranin-O/Fast Green histology images of TMJs at 3 weeks after the UAC and Sham procedures operated on 3-month-old female wild-type (+/+) and *Col5a1*$^{+/-}$ (+/–) mice. b) Zoom-in histology images highlight the tissue thickening and high cellularity of condylar cartilage at the posterior end, and the absence of appreciable changes in articular disc. c) Modified Mankin score for UAC and Sham-operated +/+ and +/– TMJs (mean ± 95% CI, $n = 5$ for each genotype and procedure type, *: $p < 0.05$ between genotypes, $^{\#}$: $p < 0.05$ versus Sham procedure, n.s.: not significant). Each data point represents the average value measured from one animal. A complete list of statistical analysis outcomes for modified Mankin score is summarized in Table S6.

(Figs. 7, 8b). This suggested that, at the histological level, the disc was less sensitive to altered occlusal loading than condylar cartilage in the postnatal TMJ. On the mechanics front, for WT discs, the UAC group showed reduced modulus than the Sham group only at the posterior end of the inferior side, but not in other regions (Fig. 10). For *Col5a1*$^{+/-}$ discs, UAC resulted in no significant biomechanical changes in all tested regions. Comparing the two genotypes, for the Sham group, *Col5a1*$^{+/-}$ discs showed lower modulus than the WT at the posterior end on both sides and the anterior end on the inferior side, but not in other regions, similar to the moderate mechanical phenotypic changes in 3-month-old unoperated mice (Fig. 4c). For the UAC group, there were no genotype-associated differences. Together, these observations supported that articular disc was less sensitive than condylar cartilage to altered occlusal loading, with or without the reduction of collagen V.

4. Discussion

4.1. Distinct regulatory roles of collagen V in the postnatal growth of articular disc and condylar cartilage

This study highlights the distinct roles of collagen V in regulating the structure and function of articular disc versus condylar cartilage during postnatal growth (Fig. 11). These differences are manifested through the differential impacts of collagen V loss on cell fate, matrix organization and biomechanical properties within these two units, although both are considered to be fibrocartilage [45]. Specifically, in condylar cartilage, loss of collagen V leads to reduced cell density (Fig. 2c), decreased cell proliferation (Ki-67 staining, Fig. 6a,b) and Wnt/β-catenin activities (Fig. 6c,d), as well as significantly reduced tissue modulus. Also, these changes are present not only in the central region [27] but also throughout the

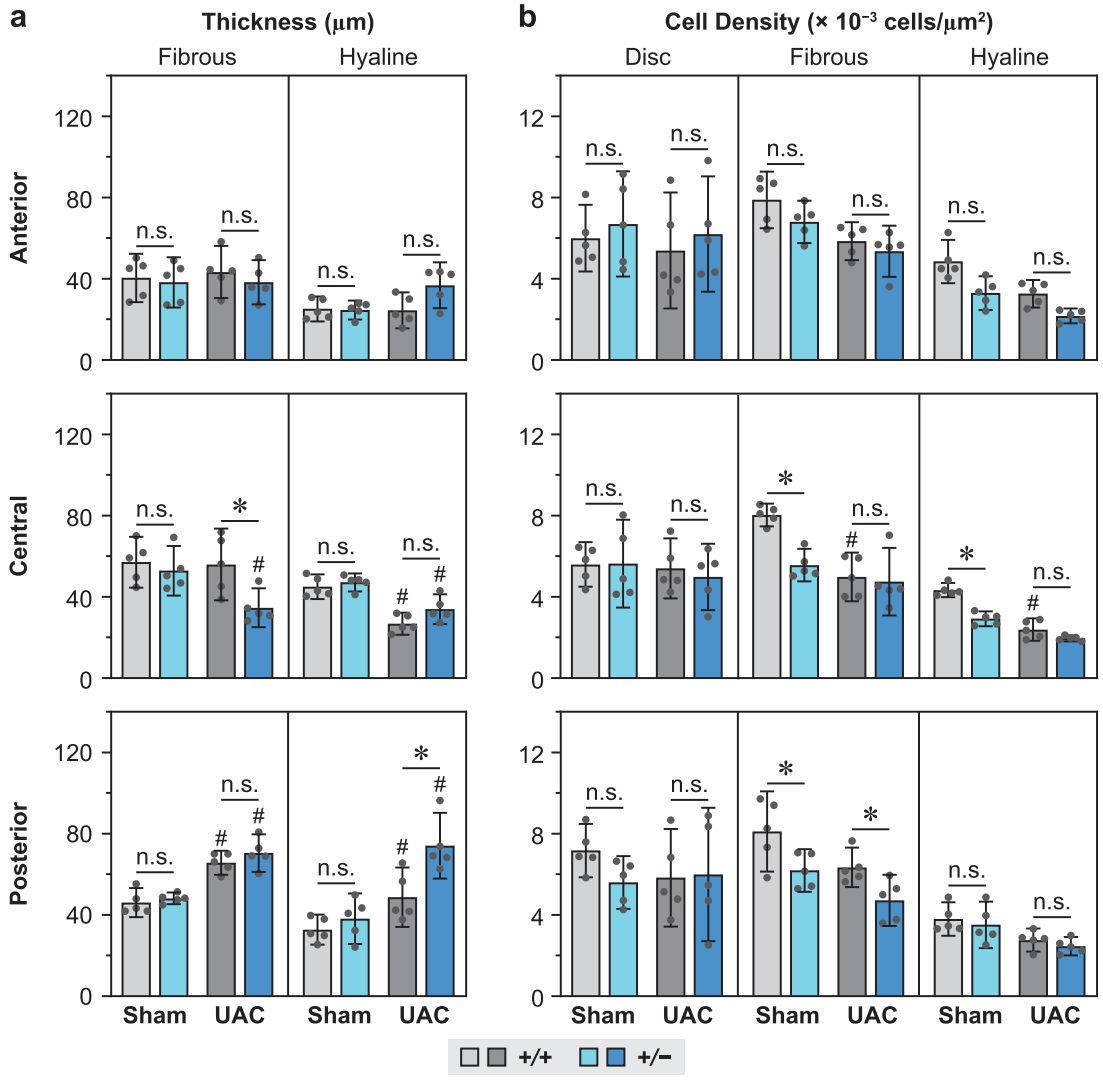

Fig. 8. Comparisons of a) the thickness of each condylar cartilage layer and b) the cell density within the disc and each condylar cartilage layer at 3 weeks after UAC and Sham procedures applied to 3-month-old female wild-type (+/+) and *Col5a1*$^{+/-}$ (+/−) mice (mean ± 95% CI, $n = 5$, *: $p < 0.05$ between genotypes, #: $p < 0.05$ versus Sham procedure, n.s.: not significant). Each data point represents the average value measured from one animal. A complete list of statistical analysis outcomes for condylar cartilage layer thickness and cell density is summarized in Table S7 and S8, respectively.

anterior and posterior ends, underscoring the crucial role of collagen V in maintaining condylar cartilage cell fate. These impacts can be attributed to the presence of highly proliferative, multipotent progenitors in the polymorphic zone of condylar fibrous layer [46,47]. During postnatal growth, these cells undergo active proliferation and chondrogenic differentiation, giving rise to the underlying hyaline cartilage [48]. Here, we show that collagen V is highly expressed in the fibrous layer, corroborating its hypothesized role in mediating the residing progenitor cells [27]. To this end, one limitation of this study is that we have not yet delineated the biological or mechanobiological axis by which collagen V regulates the progenitor cell activities at different stages of development, growth and disease. Recent studies have highlighted several specific traits of condylar progenitors, including its high expression of stem cell marker α-SMA (*Acta2*) [46] and the Wnt-inhibitory gene *Lgr5* [49]. During TMJ maturation, an intricately balanced Wnt/β-catenin signaling is required for normal condylar cartilage growth and maintenance, where both loss-of-function [50] and gain-of-function [49,51,52] of β-catenin leads to reduced cell proliferation and impaired hyaline cartilage formation, and modulating Wnt signaling in injured TMJ shows promises in ameliorating cartilage degeneration [49]. Meanwhile, our results clearly support a role for collagen V in mediating the Wnt/β-catenin activities of condylar progenitors (Fig. 6c,d). Our ongoing studies aim to pinpoint the age- and disease-specific roles of collagen V in regulating the matrix turnover and cell-matrix crosstalk of these progenitors using conditional Cre drivers that specifically target cells in condylar cartilage, such as the chondrocyte-specific *AcanCre*^{ER} model [53].

For articular disc, although it is considered to contain fibroblast-like and chondrocyte-like cells [54] with multi-differential potential when cultured *in vitro* [55,56], we show that these cells are different from the condylar progenitors. Specifically, most disc cells adapt a more elongated, fibroblast-like morphology with significantly higher NARs than those of the more rounded condylar progenitors (Fig. 2d). A recent study shows that even in newborn mice, the majority of disc cells are classified as fibroblasts, of which, only a subset retains the chondrogenic potential [57]. Although a small cluster of *Notch3*/*Thy1*-expressing mural cells identified in the anterior end demonstrates multipotent progenitor traits, these cells gradually lose their progenitor characteristics and become fibroblasts during maturation [57]. Thus, in postnatal TMJ, the majority of disc cells have likely

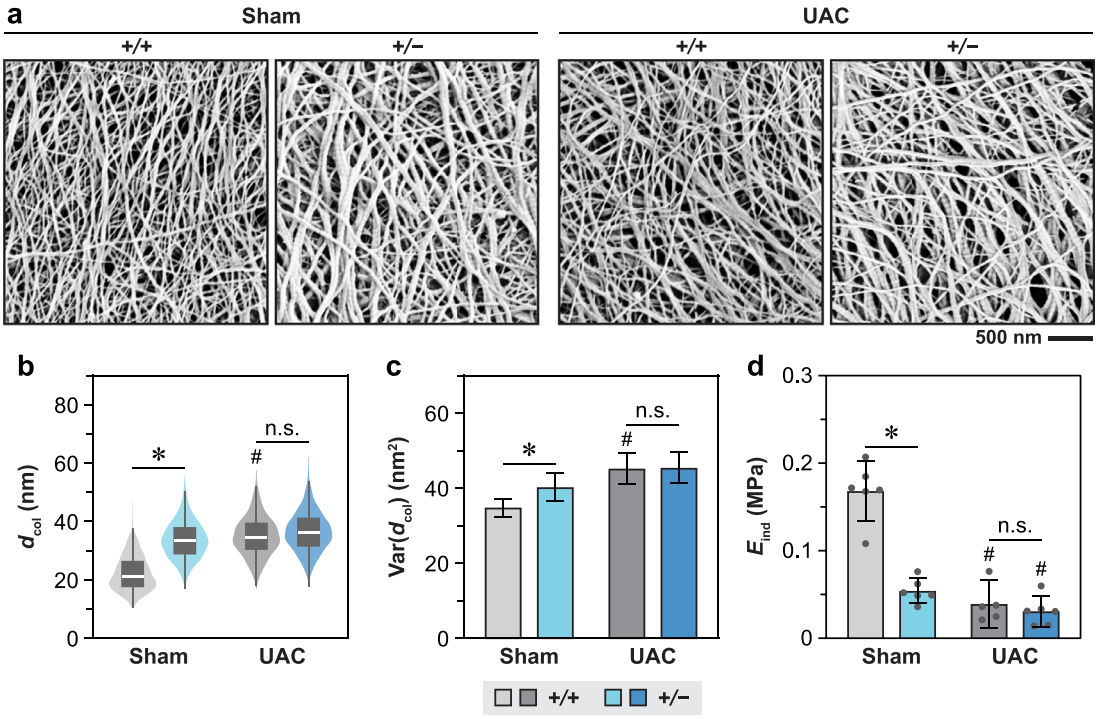

Fig. 9. Alterations of TMJ condylar cartilage surface collagen fibril nanostructure and biomechanical properties following UAC-induced remodeling. a) Representative SEM images of condylar cartilage surface at 3 weeks after UAC and Sham procedures on 3-month-old female wild-type (+/+) and *Col5a1*$^{+/-}$ (+/−) mice. b-d) Comparisons of b) collagen fibril diameter, d_{col}, distribution (violin plots), c) heterogeneity (variance, mean ± 95% CI, > 100 fibrils from $n = 3$ mice for each genotype) and d) indentation modulus, E_{ind} (MPa, mean ± 95% CI, $n = 5$) between +/+ and +/− mice (*: $p < 0.05$, #: $p < 0.05$ versus Sham procedure, n.s.: not significant). Panel d: Each data point represents the average value measured from one animal. A complete list of statistical analysis outcomes for d_{col} and E_{ind} is summarized in Tables S9 and S6, respectively.

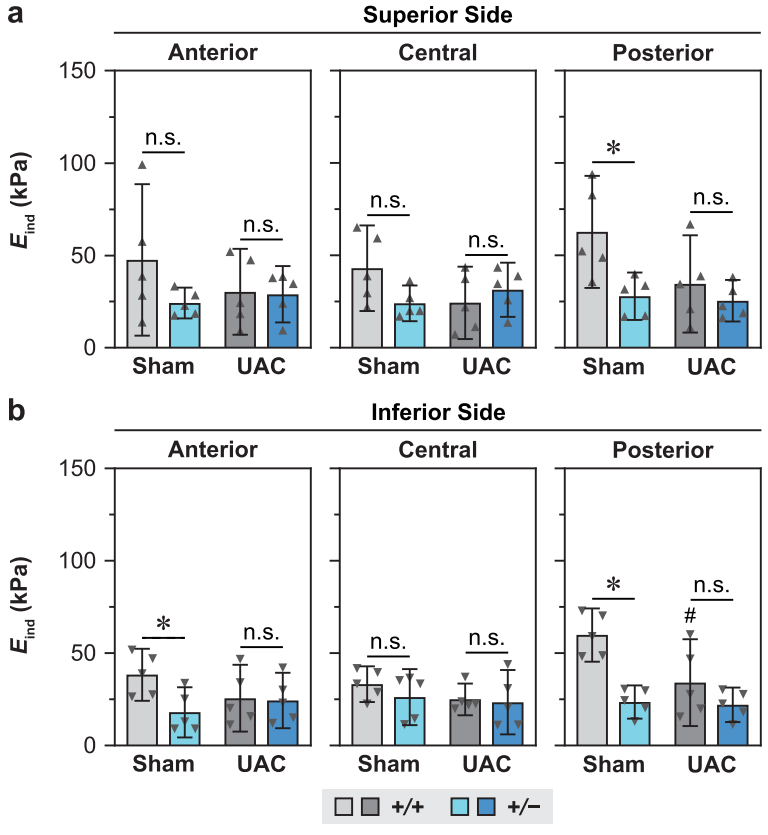

Fig. 10. Comparison of the indentation modulus, E_{ind} (kPa), of articular disc at 3 weeks after UAC and Sham procedures applied to 3-month-old female wild-type (+/+) and *Col5a1*$^{+/-}$ (+/−) mice, a) superior side, b) inferior side (mean ± 95% CI, $n = 5$, *: $p < 0.05$, #: $p < 0.05$ versus Sham procedure, n.s.: not significant). Each data point represents the average value measured from one animal. A complete list of statistical analysis outcomes for E_{ind} is summarized in Tables S10.

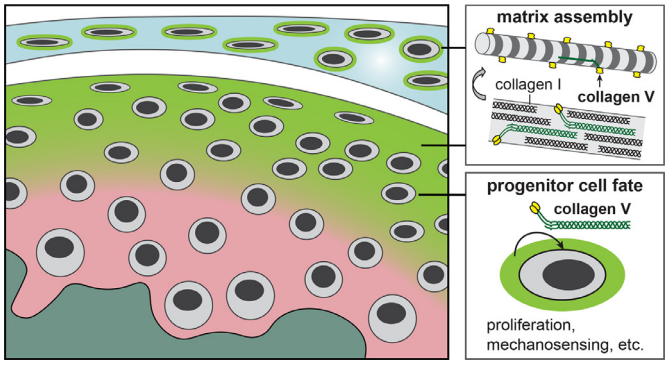

Fig. 11. Schematic illustration of the working hypothesis on the distinct roles of collagen V in regulating the TMJ articular disc versus condylar cartilage, inspired by and extended from Ref. [27]. For postnatal TMJs, in condylar cartilage, collagen V is highly concentrated in the fibrous layer. In addition to its mediation of ECM collagen fibril assembly, collagen V also regulates the proliferation, fate and mechanobiological responses of progenitor cells in the fibrous layer. In contrast, the disc does not contain a large population of these progenitors, and contains much less collagen V localized in the pericellular domain. In the disc, collagen V does not have a pronounced impact on cell fate or mechanoresponses, and its primary role is to regulate the assembly and structure of collagen I fibrils.

differentiated into the fibroblast-like lineage and do not retain the progenitor traits as condylar cartilage cells, which is supported by the minimal expressions of Ki-67 and β-catenin in the disc of 1-month-old TMJ (Fig. 6a,c). Meanwhile, our observation that disc cells express much less collagen V than condylar progenitors (Fig. 1a) corroborate a lesser role of collagen V in regulating the disc cells.

On the matrix front, the abnormal thickening of collagen fibrils throughout all tested regions in *Col5a1*$^{+/-}$ disc (Figs. 3, 4a,b) supports that collagen V retains its canonical role of regulating collagen I fibrillogenesis [17] and limiting aberrant fibril lateral growth [18] in the disc. On the other hand, reduction of collagen V impacts the disc modulus only at the posterior end (Figs. 4c, 5b), which may seem contradictory to the ubiquitous increase in fibril diameter and heterogeneity observed throughout all tested regions (Fig. 4a,b). This could be associated with the high degree of structural heterogeneity and complexity of the disc collagenous matrix (Fig. 3). As mechanical properties of biological tissues represent integrated responses of matrix composition and assembly [58], many factors, including the cross-linking, diameter, alignment and the pre-tensed state of collagen fibrils, could impact the local modulus of articular disc. During physiologic loading, the disc sustains extensive tensile and shear stresses, primarily along the anteroposterior direction [59], which could direct the formation of larger collagen fibril bundles along this direction, especially on the superior surface (Fig. 3a). On the other hand, the inferior side, particularly the central region, sustains more compressive stresses to enhance disc-condyle congruency and reduce point contact stress [60], which corroborate the presence of thinner, less aligned fibrils (Fig. 3) and lower modulus (Fig. 4c). This complex loading pattern thus contributes to the formation of the heterogeneous structure on disc surfaces with a mixture of random, thinner fibrils and aligned, thicker fibril bundles (Fig. 3). Although loss of collagen V leads to fibril thickening in general, its influence on fibril cross-linking, alignment and tensile stresses could vary substantially with tissue region and loading patterns. Changes in these factors could be further complicated by the altered mechanical adaptation of the *Col5a1*$^{+/-}$ disc, as the impaired condylar cartilage mechanical properties are expected to disrupt the disc-condyle contact mechanics. Thus, with the loss of collagen V, other structural and mechanical factors could outweigh the effects of fibril thickening, resulting in varied impacts on the local mechanical properties within different regions of the disc (Fig. 4c). To this end, the moderate differences in the biomechanical phenotype of 1- and 2-month-old *Col5a1*^{iKO} discs (Fig. 5b) relative to the 3-month-old *Col5a1*$^{+/-}$ model (Fig. 4c) can be attributed to age-related differences in the loading pattern that the disc sustains, as well as the differences in the degree of collagen V loss in these two models. In contrast to the complex fibrillar structure of the disc surface, the surface of condylar cartilage is characterized by a transverse isotropic fibril mesh typical of compression-bearing cartilage surfaces, despite the inherent heterogeneity throughout the tissue bulk [61]. With a similar fibril thickening effect, loss of collagen V has a more pronounced impact on the modulus reduction of condylar cartilage [27], further supporting the lesser role of collagen V in maintaining the overall integrity of the disc (Fig. 11).

4.2. Role of collagen V in aberrant occlusal loading-induced TMJ remodeling

We also underscore the high sensitivity of condylar cartilage to occlusal loading, and the pivotal role of collagen V in mediating the cell mechanoresponses. For UAC-operated WT condyles, the reduced sGAG staining, altered tissue morphology and cell density, increased Mankin score, thickened collagen fibrils and decreased modulus in the central region (Figs. 7, 8) clearly evidence the degenerative changes of condylar cartilage in response to altered loading. Meanwhile, the increased sGAG staining and tissue thickening at the posterior end (Figs. 7, 8a) suggest that while UAC-induced aberrant occlusal loading likely inhibits chondrogenic differentiation in the central region, it activates abnormal chondrogenic activities and cell anabolism, resulting in abnormal tissue hypertrophy at the posterior end. This is likely a result of the shift in occlusal loading, which leads to reduced compressive forces in the central region but increased forces at the posterior end, induced by the unilateral anterior crossbite prosthesis. In this process, the importance of collagen V is hallmarked by the elevated condylar cartilage responses in *Col5a1*$^{+/-}$ mice, including higher Mankin scores indicating accelerated remodeling, and more substantial tissue hypertrophy and cell clustering at the posterior end (Fig. 7b). These differences thus support a pivotal role of collagen V in mediating the mechanobiology of condylar progenitors during remodeling. To this end, although studying the *Col5a1*$^{+/-}$ model provides direct insights into the higher propensity toward TMJ in cEDS patients, one limitation of this constitutive collagen V haploinsufficiency model is that the observed degenerative phenotype arises from combined effects of impaired development and altered responses to aberrant loading. We thus cannot delineate the role of collagen V in UAC-induced remodeling versus postnatal growth in these mice. To address this challenge, our ongoing studies aim to pinpoint the role of collagen V in remodeling by studying the impact of conditional cartilage-specific collagen V knockout using the *AcanCre*^{ER} model [53], and to elucidate the molecular mechanisms by which collagen V regulates the condylar progenitor cell mechanobiology and matrix assembly.

The lack of biomechanical phenotype in the disc (Fig. 10) is also contrasting to the response of condylar cartilage (Fig. 9d). This could again be associated with the more differentiated, mature cell type in the disc, rendering reduced sensitivity to changes in mechanical stimuli and/or the integrity of matrix microniche. Unlike condylar cartilage that continues to undergo mechanically regulated chondrogenesis during postnatal growth, the disc retains its nature of fibrogenic tissue throughout lifespan. In soft connective tissues such as knee cartilage, the turnover of proteoglycans is much faster than that of collagens [62,63]. Although the turnover rate of disc matrix collagens has not been quantified, it is expected to be slower than that of the more proteoglycan-rich condylar cartilage. These factors could contribute to the minimal response of

the disc to UAC-induced aberrant loading in both genotypes. Similarly, in murine knee cartilage, when post-traumatic osteoarthritis is induced by the destabilization of the medial meniscus (DMM) surgery, degeneration of cartilage precedes changes of other tissues, including the meniscus, its fibrocartilaginous loading counterpart [64,65]. Taken together, we show that condylar cartilage is more susceptible to degeneration than the disc, induced either by aberrant loading, or deficiency of collagen V. Therefore, condylar cartilage is more likely to be the site of TMJ disease initiation and could play a central role in the higher propensity to TMJ disorders amongst cEDS patients [26].

4.3. Implications for articular disc and condylar cartilage regeneration

One guiding blueprint for tissue engineering is to recapitulate the key steps of native tissue development, thereby restoring the structure and function of the native tissues [66]. As highlighted by this work, articular disc and condylar cartilage have composition, structure and dynamic cell-matrix crosstalk distinctive to each tissue. This indicates that knowledge derived from other tissues, such as knee cartilage and meniscus, are not directly translatable for designing regeneration strategies for the TMJ. A number of previous studies have aimed at uncovering the roles of individual matrix molecules in condylar cartilage by evaluating the phenotype of genetic knockout or knockdown mice, including biglycan/fibromodulin [67-69], lubricin (Prg4) [70-72], tenascin-C [73], lysyl oxidase-like 2 (LOXL2) [74], as well as collagens II [75], VI [76], IX [77] and XI [77,78]. For articular disc, there has been limited attempts in studying its matrix, except for the work highlighting aberrant disc thickening in *Prg4*$^{-/-}$ mice [72]. Findings from this study, including the roles of collagen V, local heterogeneity in collagen fibril architecture and micromechanics, as well as high mechanoadaptative responses of condylar cartilage, can integrate with these previous studies, contributing to the fundamental understanding of the ECM formation, remodeling and degradation of the TMJ. Building on this work, our future studies aim to uncover the activities of collagens V and XI, the two highly homologous molecules that regulate the initial assembly of collagens I and II, respectively [16]. Given their synergy in tendons [79], it is likely that these two molecules could have individual as well as coordinated roles in regulating these two TMJ tissues, especially the fibro-hyaline hybrid condylar cartilage. Furthermore, results from this work could serve as a benchmark for designing novel regeneration strategies for restoring the biomechanical functions of condylar cartilage and articular disc as well as modulating cell-matrix interactions using collagen V as a new biomaterial candidate or gene therapy target. In this regard, it is worth noting that there are salient differences in the anatomy and structure of TMJs between mice, humans and other larger animals [80,81], which could limit the direct translation of the findings from the current study. However, molecular and structural insights generated by this work, as well as the application of AFM-based nanomechanical methods, can be extended for studying the TMJs of larger animal models.

5. Conclusions

This study underscores the distinct activities of collagen V in regulating the TMJ articular disc versus condylar cartilage during postnatal growth and remodeling (Fig. 11). Although both are considered fibrocartilage, the articular disc does not contain a population of the proliferative progenitors that express high levels of collagen V during postnatal growth. As a result, the impact of collagen V loss on articular disc is limited to the thickening of collagen fibrils and local modulus reduction at the posterior end, which is in stark contrast to the substantial changes in cell proliferation/clustering, tissue morphology and matrix modulus observed in condylar cartilage. When *in vivo* occlusal loading is altered by the UAC model, loss of collagen V aggravates the remodeling of condylar cartilage, as marked by higher Mankin scores, collagen fibril thickening, modulus reduction, and aberrant tissue hypertrophy at the posterior end. In contrast, UAC leads to only moderate changes of the disc micromodulus at the posterior end, and deficiency of collagen V has minimal impact on the response. Taken together, the more mature cell phenotype, heterogeneous structure and complex loading pattern of articular disc could contribute to the less pronounced, region-dependent role of collagen V in regulating its structure and biomechanical properties. These results provide a structure-function basis for designing new biomaterial scaffolds and tissue engineering approach for the repair of articular disc and condylar cartilage through modulating the activities of collagen V.

Declaration of competing interests

The authors declare that they have no known competing financial interests or personal relationships that could have appeared to influence the work reported in this paper.

CRediT authorship contribution statement

Prashant Chandrasekaran: Data curation, Formal analysis, Investigation, Methodology, Validation, Visualization, Writing – original draft, Writing – review & editing. **Abdulaziz Alanazi:** Data curation, Formal analysis, Investigation, Methodology, Writing – review & editing. **Bryan Kwok:** Data curation, Formal analysis, Investigation, Methodology, Visualization, Writing – original draft, Writing – review & editing. **Qing Li:** Data curation, Methodology, Writing – review & editing. **Girish Viraraghavan:** Data curation, Writing – review & editing, Methodology. **Sriram Balasubramanian:** Data curation, Methodology, Writing – review & editing. **David B. Frank:** Data curation, Methodology, Writing – review & editing. **X. Lucas Lu:** Data curation, Methodology, Writing – review & editing. **David E. Birk:** Data curation, Methodology, Writing – review & editing. **Robert L. Mauck:** Data curation, Methodology, Writing – review & editing, Conceptualization, Funding acquisition, Investigation. **Nathaniel A. Dyment:** Data curation, Methodology, Writing – review & editing, Conceptualization, Funding acquisition, Investigation. **Eiki Koyama:** Data curation, Methodology, Writing – review & editing, Conceptualization, Funding acquisition, Investigation. **Lin Han:** Conceptualization, Data curation, Formal analysis, Funding acquisition, Investigation, Methodology, Resources, Supervision, Validation, Visualization, Writing – original draft, Writing – review & editing.

Acknowledgements

This work was financially supported by the National Science Foundation (NSF) Grant CMMI-1751898 (to LH), National Institutes of Health (NIH) Grant R21DE029567 (to LH), as well as NIH Grant P30AR069619 to the Penn Center for Musculoskeletal Disorders. We thank Dr. L. J. Soslowsky (University of Pennsylvania) for the kind help with murine TMJ samples.

Supplementary materials

Supplementary material associated with this article can be found, in the online version, at doi:10.1016/j.actbio.2024.09.046.

References

[1] W.E. Roberts, C.J. Goodacre, The temporomandibular joint: a critical review of life-support functions, development, articular surfaces, biomechanics and degeneration, J. Prosthodont. 29 (2020) 772–779.
[2] S. Ingawalé, T. Goswami, Temporomandibular joint: disorders, treatments, and biomechanics, Ann. Biomed. Eng. 37 (2009) 976–996.
[3] Prevalence of TMJD and its Signs and Symptoms. 2018. National institute of dental and craniofacial research. https://www.nidcr.nih.gov/research/data-statistics/facial-pain/prevalence.
[4] X.D. Wang, J.N. Zhang, Y.H. Gan, Y.H. Zhou, Current understanding of pathogenesis and treatment of TMJ osteoarthritis, J. Dent. Res. 94 (2015) 666–673.
[5] A.R. Chin, J. Gao, Y. Wang, J.M. Taboas, A.J. Almarza, Regenerative potential of various soft polymeric scaffolds in the temporomandibular joint condyle, J. Oral Maxillofac. Surg. 76 (2018) 2019–2026.
[6] T.M. Acri, K. Shin, D. Seol, N.Z. Laird, I. Song, S.M. Geary, J.L. Chakka, J.A. Martin, A.K. Salem, Tissue engineering for the temporomandibular joint, Adv. Healthc. Mater. 8 (2019) e1801236.
[7] E. Tanaka, J.H. Koolstra, Biomechanics of the temporomandibular joint, J. Dent. Res. 87 (2008) 989–991.
[8] M.S. Detamore, K.A. Athanasiou, Structure and function of the temporomandibular joint disc: implications for tissue engineering, J. Oral Maxillofac. Surg. 61 (2003) 494–506.
[9] K.D. Allen, K.A. Athanasiou, Viscoelastic characterization of the porcine temporomandibular joint disc under unconfined compression, J. Biomech. 39 (2006) 312–322.
[10] P. Chandrasekaran, B. Doyran, Q. Li, B. Han, T.E. Bechtold, E. Koyama, X.L. Lu, L. Han, Biomechanical properties of murine TMJ articular disc and condyle cartilage via AFM-nanoindentation, J. Biomech. 60 (2017) 134–141.
[11] M. Singh, M.S. Detamore, Tensile properties of the mandibular condylar cartilage, J. Biomech. Eng. 130 (2008) 011009.
[12] L. Han, A.J. Grodzinsky, C. Ortiz, Nanomechanics of the cartilage extracellular matrix, Annu. Rev. Mater. Res. 41 (2011) 133–168.
[13] E.A. Makris, P. Hadidi, K.A. Athanasiou, The knee meniscus: structure-function, pathophysiology, current repair techniques, and prospects for regeneration, Biomaterials 32 (2011) 7411–7431.
[14] S. Wadhwa, S. Kapila, TMJ disorders: future innovations in diagnostics and therapeutics, J. Dent. Educ. 72 (2008) 930–947.
[15] M.K. Murphy, R.F. MacBarb, M.E. Wong, K.A. Athanasiou, Temporomandibular disorders: a review of etiology, clinical management, and tissue engineering strategies, Int. J. Oral Maxillofac. Implants 28 (2013) e393–e414.
[16] D.E. Birk, P. Brückner, Collagens, suprastructures, and collagen fibril assembly, in: R.P. Mecham (Ed.), The Extracellular Matrix: an Overview, Springer-Verlag, Berlin, 2011, pp. 77-115.
[17] R.J. Wenstrup, J.B. Florer, E.W. Brunskill, S.M. Bell, I. Chervoneva, D.E. Birk, Type V collagen controls the initiation of collagen fibril assembly, J. Biol. Chem. 279 (2004) 53331–53337.
[18] T.F. Linsenmayer, E. Gibney, F. Igoe, M.K. Gordon, J.M. Fitch, L.I. Fessler, D.E. Birk, Type V collagen: molecular structure and fibrillar organization of the chicken α1(V) NH_2-terminal domain, a putative regulator of corneal fibrillogenesis, J. Cell Biol. 121 (1993) 1181–1189.
[19] M. Sun, S. Chen, S.M. Adams, J.B. Florer, H. Liu, W.W. Kao, R.J. Wenstrup, D.E. Birk, Collagen V is a dominant regulator of collagen fibrillogenesis: dysfunctional regulation of structure and function in a corneal-stroma-specific Col5a1-null mouse model, J. Cell Sci. 124 (2011) 4096–4105.
[20] B.K. Connizzo, S.M. Adams, T.H. Adams, D.E. Birk, L.J. Soslowsky, Collagen V expression is crucial in regional development of the supraspinatus tendon, J. Orthop. Res. 34 (2016) 2154–2161.
[21] B.K. Connizzo, L. Han, D.E. Birk, L.J. Soslowsky, Collagen V-heterozygous and -null supraspinatus tendons exhibit altered dynamic mechanical behaviour at multiple hierarchical scales, Interface Focus 6 (2016) 20150043.
[22] J. DeNigris, Q. Yao, E.K. Birk, D.E. Birk, Altered dermal fibroblast behavior in a collagen V haploinsufficient murine model of classic Ehlers-Danlos syndrome, Connect. Tissue Res. 57 (2016) 1–9.
[23] K. Machol, U. Polak, M. Weisz-Hubshman, I.W. Song, S. Chen, M.M. Jiang, Y. Chen-Evenson, M.A.E. Weis, D.R. Keene, D.R. Eyre, B.H. Lee, Molecular alterations due to Col5a1 haploinsufficiency in a mouse model of classic Ehlers-Danlos syndrome, Hum. Mol. Genet. 31 (2022) 1325–1335.
[24] T. Yokota, J. McCourt, F. Ma, S. Ren, S. Li, T.H. Kim, Y.Z. Kurmangaliyev, R. Nasiri, S. Ahadian, T. Nguyen, X.H.M. Tan, Y. Zhou, R. Wu, A. Rodriguez, W. Cohn, Y. Wang, J. Whitelegge, S. Ryazantsev, A. Khademhosseini, M.A. Teitell, P.Y. Chiou, D.E. Birk, A.C. Rowat, R.H. Crosbie, M. Pellegrini, M. Seldin, A.J. Lusis, A. Deb, Type V collagen in scar tissue regulates the size of scar after heart injury, Cell 182 (2020) 545–562 e523.
[25] F. Malfait, R.J. Wenstrup, A. De Paepe, Clinical and genetic aspects of Ehlers–Danlos syndrome, classic type, Genet. Med. 12 (2010) 597–605.
[26] L.A. Norton, L.A. Assael, Orthodontic and temporomandibular joint considerations in treatment of patients with Ehlers-Danlos syndrome, Am. J. Orthod. Dentofacial Orthop. 111 (1997) 75–84.
[27] P. Chandrasekaran, B. Kwok, B. Han, S.M. Adams, C. Wang, D.R. Chery, R.L. Mauck, N.A. Dyment, X.L. Lu, D.B. Frank, E. Koyama, D.E. Birk, L. Han, Type V collagen regulates the structure and biomechanics of TMJ condylar cartilage: a fibrous-hyaline hybrid, Matrix Biol. 102 (2021) 1–19.
[28] M. Sun, B.K. Connizzo, S.M. Adams, B.R. Freedman, R.J. Wenstrup, L.J. Soslowsky, D.E. Birk, Targeted deletion of collagen V in tendons and ligaments results in a classic Ehlers-Danlos syndrome joint phenotype, Am. J. Pathol. 185 (2015) 1436–1447.
[29] G. Shen, M.A. Darendeliler, The adaptive remodeling of condylar cartilage - a transition from chondrogenesis to osteogenesis, J. Dent. Res. 84 (2005) 691–699.
[30] A. Utreja, N.A. Dyment, S. Yadav, M.M. Villa, Y. Li, X. Jiang, R. Nanda, D.W. Rowe, Cell and matrix response of temporomandibular cartilage to mechanical loading, Osteoarthritis Cartilage 24 (2016) 335–344.
[31] R. Kaul, M.H. O'Brien, E. Dutra, A. Lima, A. Utreja, S. Yadav, The effect of altered loading on mandibular condylar cartilage, PLoS One 11 (2016) e0160121.
[32] D.A. Reed, Y. Zhao, M. Han, L.G. Mercuri, M. Miloro, Mechanical loading disrupts focal adhesion kinase activation in mandibular fibrochondrocytes during murine temporomandibular joint osteoarthritis, J. Oral Maxillofac. Surg. 79 (2021) 2058.e2051-2058.e2015.
[33] Y.L. Wang, J. Zhang, M. Zhang, L. Lu, X. Wang, M. Guo, X. Zhang, M.Q. Wang, Cartilage degradation in temporomandibular joint induced by unilateral anterior crossbite prosthesis, Oral Dis. 20 (2014) 301–306.
[34] Y.D. Liu, L.F. Liao, H.Y. Zhang, L. Lu, K. Jiao, M. Zhang, J. Zhang, J.J. He, Y.P. Wu, D. Chen, M.Q. Wang, Reducing dietary loading decreases mouse temporomandibular joint degradation induced by anterior crossbite prosthesis, Osteoarthritis Cartilage 22 (2014) 302–312.
[35] L. Xu, I. Polur, C. Lim, J.M. Servais, J. Dobeck, Y. Li, B.R. Olsen, Early-onset osteoarthritis of mouse temporomandibular joint induced by partial discectomy, Osteoarthritis Cartilage 17 (2009) 917–922.
[36] T. Scholzen, J. Gerdes, The Ki-67 protein: from the known and the unknown, J. Cell. Physiol. 182 (2000) 311–322.
[37] B. Han, Q. Li, C. Wang, P. Patel, S.M. Adams, B. Doyran, H.T. Nia, R. Oftadeh, S. Zhou, C.Y. Li, X.S. Liu, X.L. Lu, M. Enomoto-Iwamoto, L. Qin, R.L. Mauck, R.V. Iozzo, D.E. Birk, L. Han, Decorin regulates the aggrecan network integrity and biomechanical functions of cartilage extracellular matrix, ACS Nano 13 (2019) 11320–11333.
[38] E.K. Dimitriadis, F. Horkay, J. Maresca, B. Kachar, R.S. Chadwick, Determination of elastic moduli of thin layers of soft material using the atomic force microscope, Biophys. J. 82 (2002) 2798–2810.
[39] K.W. Kim, M.E. Wong, J.F. Helfrick, J.B. Thomas, K.A. Athanasiou, Biomechanical tissue characterization of the superior joint space of the porcine temporomandibular joint, Ann. Biomed. Eng. 31 (2003) 924–930.
[40] C.K. Hagandora, T.W. Chase, A.J. Almarza, A comparison of the mechanical properties of the goat temporomandibular joint disc to the mandibular condylar cartilage in unconfined compression, J. Dent. Biomech. (2011) 212385 2011.
[41] D. Bates, M. Mächler, B. Bolker, S. Walker, Fitting linear mixed-effects models using lme4, J. Stat. Softw. 67 (1) (2015) 1–48.
[42] S. Holm, A simple sequentially rejective multiple test procedure, Scand. J. Statist. 6 (1979) 65–70.
[43] J.A. Petruska, A.J. Hodge, A subunit model for the tropocollagen macromolecule, in: Proc. Natl. Acad. Sci. USA, 51, 1964, pp. 871–876.
[44] Q. Li, B. Han, C. Wang, W. Tong, W.J. Tseng, L.-H. Han, X.S. Liu, M. Enomoto-Iwamoto, R.L. Mauck, L. Qin, R.V. Iozzo, D.E. Birk, L. Han, Mediation of cartilage matrix degeneration and fibrillation by decorin in post-traumatic osteoarthritis, Arthritis Rheumatol. 72 (2020) 1266–1277.
[45] B.K. Zimmerman, E.D. Bonnevie, M. Park, Y. Zhou, L. Wang, D.L. Burris, X.L. Lu, Role of interstitial fluid pressurization in TMJ lubrication, J. Dent. Res. 94 (2015) 85–92.
[46] M.C. Embree, M. Chen, S. Pylawka, D. Kong, G.M. Iwaoka, I. Kalajzic, H. Yao, C. Shi, D. Sun, T.J. Sheu, D.A. Koslovsky, A. Koch, J.J. Mao, Exploiting endogenous fibrocartilage stem cells to regenerate cartilage and repair joint injury, Nat. Commun. 7 (2016) 13073.
[47] R. Bi, Q. Yin, J. Mei, K. Chen, X. Luo, Y. Fan, S. Zhu, Identification of human temporomandibular joint fibrocartilage stem cells with distinct chondrogenic capacity, Osteoarthritis Cartilage 28 (2020) 842–852.
[48] N. Kurio, C. Saunders, T.E. Bechtold, I. Salhab, H.D. Nah, S. Sinha, P.C. Billings, M. Pacifici, E. Koyama, Roles of Ihh signaling in chondroprogenitor function in postnatal condylar cartilage, Matrix Biol. 67 (2018) 15–31.
[49] A. Ruscitto, P. Chen, I. Tosa, Z. Wang, G. Zhou, I. Safina, R. Wei, M.M. Morel, A. Koch, M. Forman, G. Reeve, M.K. Lecholop, M. Wilson, D. Bonthius, M. Chen, M. Ono, T.C. Wang, H. Yao, M.C. Embree, Lgr5-expressing secretory cells form a Wnt inhibitory niche in cartilage critical for chondrocyte identity, Cell Stem Cell 30 (2023) 1179–1198 e1177.
[50] Y. Jing, J. Jing, K. Wang, K. Chan, S.E. Harris, R.J. Hinton, J.Q. Feng, Vital roles of β-catenin in trans-differentiation of chondrocytes to bone cells, Int. J. Biol. Sci. 14 (2018) 1–9.
[51] M. Wang, S. Li, W. Xie, J. Shen, H.J. Im, J.D. Holz, M. Wang, T.G. Diekwisch, D. Chen, Activation of β-catenin signalling leads to temporomandibular joint defects, Eur. Cell. Mater. 28 (2014) 223–235.
[52] T. Hui, Y. Zhou, T. Wang, J. Li, S. Zhang, L. Liao, J. Gu, L. Ye, L. Zhao, D. Chen, Activation of β-catenin signaling in aggrecan-expressing cells in temporomandibular joint causes osteoarthritis-like defects, Int. J. Oral Sci. 10 (2018) 13.
[53] S.P. Henry, C.W. Jang, J.M. Deng, Z. Zhang, R.R. Behringer, B. de Crombrugghe, Generation of aggrecan-CreERT2 knockin mice for inducible Cre activity in adult cartilage, Genesis 47 (2009) 805–814.
[54] M.S. Detamore, J.N. Hegde, R.R. Wagle, A.J. Almarza, D. Montufar-Solis, P.J. Duke, K.A. Athanasiou, Cell type and distribution in the porcine temporomandibular joint disc, J. Oral Maxillofac. Surg. 64 (2006) 243–248.
[55] K.J. Weekes, P. Lam, C. Kim, B. Johnstone, Characterization of temporomandibular joint articular disc progenitor cell clones, Eur. Cell. Mater. 45 (2023) 1–13.

[56] Y. Park, J. Hosomichi, C. Ge, J. Xu, R. Franceschi, S. Kapila, Immortalization and characterization of mouse temporomandibular joint disc cell clones with capacity for multi-lineage differentiation, Osteoarthritis Cartilage 23 (2015) 1532–1542.
[57] R. Bi, Q. Yin, H. Li, X. Yang, Y. Wang, Q. Li, H. Fang, P. Li, P. Lyu, Y. Fan, B. Ying, S. Zhu, A single-cell transcriptional atlas reveals resident progenitor cell niche functions in TMJ disc development and injury, Nat. Commun. 14 (2023) 830.
[58] C.T. Hung, G.A. Ateshian, Grading of osteoarthritic cartilage: correlations between histology and biomechanics, J. Orthop. Res. 34 (2016) 8–9.
[59] M.W. Beatty, M.J. Bruno, L.R. Iwasaki, J.C. Nickel, Strain rate dependent orthotropic properties of pristine and impulsively loaded porcine temporomandibular joint disk, J. Biomed. Mater. Res. 57 (2001) 25–34.
[60] E. Tanaka, M.S. Detamore, K. Tanimoto, N. Kawai, Lubrication of the temporomandibular joint, Ann. Biomed. Eng. 36 (2008) 14–29.
[61] N. Jiang, Z. Su, Y. Sun, R. Ren, J. Zhou, R. Bi, S. Zhu, Spatial heterogeneity directs energy dissipation in condylar fibrocartilage, Small 19 (2023) e2301051.
[62] T.M. Quinn, A.A. Maung, A.J. Grodzinsky, E.B. Hunziker, J.D. Sandy, Physical and biological regulation of proteoglycan turnover around chondrocytes in cartilage explants. Implications for tissue degradation and repair, Ann. N. Y. Acad. Sci. 878 (1999) 420–441.
[63] N. Verzijl, J. DeGroot, S.R. Thorpe, R.A. Bank, J.N. Shaw, T.J. Lyons, J.W.J. Bijlsma, F.P.J.G. Lafeber, J.W. Baynes, J.M. TeKoppele, Effect of collagen turnover on the accumulation of advanced glycation end products, J. Biol. Chem. 275 (2000) 39027–39031.
[64] B. Doyran, W. Tong, Q. Li, H. Jia, X. Zhang, C. Chen, M. Enomoto-Iwamoto, X.L. Lu, L. Qin, L. Han, Nanoindentation modulus of murine cartilage: a sensitive indicator of the initiation and progression of post-traumatic osteoarthritis, Osteoarthritis Cartilage 25 (2017) 108–117.
[65] D.R. Chery, B. Han, Q. Li, Y. Zhou, S.J. Heo, B. Kwok, P. Chandrasekaran, C. Wang, L. Qin, X.L. Lu, D. Kong, M. Enomoto-Iwamoto, R.L. Mauck, L. Han, Early changes in cartilage pericellular matrix micromechanobiology portend the onset of post-traumatic osteoarthritis, Acta Biomater. 111 (2020) 267–278.
[66] J.C. Bernhard, G. Vunjak-Novakovic, Should we use cells, biomaterials, or tissue engineering for cartilage regeneration? Stem Cell Res. Ther. 7 (2016) 56.
[67] S. Wadhwa, M.C. Embree, T. Kilts, M.F. Young, L.G. Ameye, Accelerated osteoarthritis in the temporomandibular joint of biglycan/fibromodulin double-deficient mice, Osteoarthritis Cartilage 13 (2005) 817–827.
[68] S. Wadhwa, M. Embree, L. Ameye, M.F. Young, Mice deficient in biglycan and fibromodulin as a model for temporomandibular joint osteoarthritis, Cells Tissues Organs 181 (2005) 136–143.
[69] M.C. Embree, T.M. Kilts, M. Ono, C.A. Inkson, F. Syed-Picard, M.A. Karsdal, A. Oldberg, Y. Bi, M.F. Young, Biglycan and fibromodulin have essential roles in regulating chondrogenesis and extracellular matrix turnover in temporomandibular joint osteoarthritis, Am. J. Pathol. 176 (2010) 812–826.
[70] A. Hill, J. Duran, P. Purcell, Lubricin protects the temporomandibular joint surfaces from degeneration, PLoS One 9 (2014) e106497.
[71] T.E. Bechtold, C. Saunders, C. Mundy, H. Um, R.S. Decker, I. Salhab, N. Kurio, P.C. Billings, M. Pacifici, H.D. Nah, E. Koyama, Excess BMP signaling in heterotopic cartilage forming in *Prg4*-null TMJ discs, J. Dent. Res. 95 (2016) 292–301.
[72] E. Koyama, C. Saunders, I. Salhab, R.S. Decker, I. Chen, H. Um, M. Pacifici, H.D. Nah, Lubricin is required for the structural integrity and post-natal maintenance of TMJ, J. Dent. Res. 93 (2014) 663–670.
[73] Y. Shinohara, K. Okamoto, Y. Goh, N. Kiga, I. Tojyo, S. Fujita, Inhibition of fibrous adhesion formation in the temporomandibular joint of tenascin-C knockout mice, Eur. J. Histochem. 58 (2014) 2337.
[74] M.M. Tashkandi, S.F. Alsaqer, T. Alhousami, F. Ali, Y.C. Wu, J. Shin, P. Mehra, L.M. Wolford, L.C. Gerstenfeld, M.B. Goldring, M.V. Bais, LOXL2 promotes aggrecan and gender-specific anabolic differences to TMJ cartilage, Sci. Rep. 10 (2020) 20179.
[75] M.L. Ricks, J.T. Farrell, D.J. Falk, D.W. Holt, M. Rees, J. Carr, T. Williams, B.A. Nichols, L.C. Bridgewater, P.R. Reynolds, D.L. Kooyman, R.E. Seegmiller, Osteoarthritis in temporomandibular joint of Col2a1 mutant mice, Arch. Oral Biol. 58 (2013) 1092–1099.
[76] T. Komori, Y. Ji, H. Pham, P. Jani, T.M. Kilts, V. Kram, L. Li, M.F. Young, Type VI collagen regulates endochondral ossification in the temporomandibular joint, JBMR Plus 6 (2022) e10617.
[77] N.P. Lam, Y. Li, A.B. Waldman, J. Brussiau, P.L. Lee, B.R. Olsen, L. Xu, Age-dependent increase of discoidin domain receptor 2 and matrix metalloproteinase 13 expression in temporomandibular joint cartilage of type IX and type XI collagen-deficient mice, Arch. Oral Biol. 52 (2007) 579–584.
[78] L. Xu, C.M. Flahiff, B.A. Waldman, D. Wu, B.R. Olsen, L.A. Setton, Y. Li, Osteoarthritis-like changes and decreased mechanical function of articular cartilage in the joints of mice with the chondrodysplasia gene (*cho*), Arthritis Rheum. 48 (2003) 2509–2518.
[79] M. Sun, E.Y. Luo, S.M. Adams, T. Adams, Y. Ye, S.S. Shetye, L.J. Soslowsky, D.E. Birk, Collagen XI regulates the acquisition of collagen fibril structure, organization and functional properties in tendon, Matrix Biol. 94 (2020) 77–94.
[80] R. Ren, J. Zhou, Y. Sun, W. Telha, N. Song, Y. Zhan, S. Zhu, N. Jiang, Interspecies comparison of temporomandibular joint condylar cartilage extracellular matrix from macro to microscopy, J. Mech. Behav. Biomed. Mater. 145 (2023) 106007.
[81] A.J. Almarza, B.N. Brown, B. Arzi, D.F. Ângelo, W. Chung, S.F. Badylak, M. Detamore, Preclinical animal models for temporomandibular joint tissue engineering, Tissue Eng. Part B Rev. 24 (2018) 171–178.